Chapter 2
Climate in Asia and the Pacific: Climate Variability and Change

Michael James Salinger, Madan Lall Shrestha, Ailikun, Wenjie Dong, John L. McGregor, and Shuyu Wang

Abstract The geographic extent of Asia and the Pacific leads to great variation in the climate of the region. Major influences on global climate arise from the scale and elevation of the Himalayan Tibetan Plateau (HTP), and from the air-sea interactions in the Pacific associated with the El Niño–Southern Oscillation (ENSO). The monsoon has a profound effect on the climate of Asia, with its strong seasonal cycle. Variability is also caused by ENSO, the Indian Ocean Dipole (IOD) and

M.J. Salinger (✉)
University of Auckland, 3/7 Mattson Road, Pakuranga, 2010 Auckland, New Zealand
e-mail: salinger@orcon.net.nz

M.L. Shrestha (✉)
Nepal Academy of Science and Technology, Khumaltar, Lalitpur, Nepal
e-mail: madanls1949@gmail.com

Ailikun
Institute of Atmospheric Physics, Monsoon Asia Integrated Regional Study (MAIRS)
IPO, Chinese Academy of Sciences, 40# Hua Yan Li, Qi JIa Huo Zi, Chao Yang District,
P.O. Box 9804, 100029 Beijing, China
e-mail: aili@mairs-essp.org; aili@tea.ac.cn

W. Dong
State Key Laboratory of Earth Surface Processes and Resource Ecology,
College of Global Change and Earth System Science, Beijing Normal University,
19 Xinjiekou Wai Street, 100875 Beijing, China
e-mail: dongwj@bnu.edu.cn

J.L. McGregor
CSIRO Marine and Atmospheric Research, 107-121 Station Street,
3195 Aspendale, VIC, Australia
e-mail: John.McGregor@csiro.au

S. Wang
Institute of Atmospheric Physics, Chinese Academy of Sciences,
Building 40, Huayan Li, Chaoyang District, 100029 Beijing, China
e-mail: wsy@tea.ac.cn

M.J. Manton and L.A. Stevenson (eds.), *Climate in Asia and the Pacific: Security, Society and Sustainability*, Advances in Global Change Research 56,
DOI 10.1007/978-94-007-7338-7_2,

Pacific Decadal Oscillation (PDO). ENSO is the principal source of inter-annual global climate variability. ENSO has significant climate and societal impacts on both regional and global scales. The climate effects of ENSO are modulated on decadal time scales by the PDO. IOD affects the climate in the Indian Ocean and Australasia. Climate observations show significant warming trends in temperature across Asia and the Pacific; not only is there an increase in mean temperature, but there is more warming in North Asia and less in the Pacific during the twentieth century. Observed trends in precipitation are more variable, with some evidence of increasing intensity of storms. Glacier mass balance studies show dramatic decline in ice mass in the Himalayas and New Zealand, with monitored ice mass losses of 0.3–0.5 km^2/year, in the last three decades. Temperature extremes have changed region wide: cool nights, cold days have very significantly decreased universally, and the frequency of hot days has increased. Projections of future climate change for the region suggest longer summer heat waves in South and East Asia and Australia, and increases in precipitation in several areas. Regional downscaling techniques are used to project future climate: warming is projected to be largest in high latitude (Northern Asia, Central Asia) and high altitude (Tibetan Plateau) regions; with a suppression of the south Asian summer monsoon, along with a delay of monsoon onset and increase of monsoon break periods. Monsoon precipitation is projected to increase over South Asia.

Keywords Monsoon Asia • Pacific • Climate variability trends • Climate change trends

2.1 Observed Climate Variability and Trends

2.1.1 Introduction

Asia-Pacific surface climates span a wide range of latitudes from sub-polar regimes in the Russian Federation, monsoon Asia, which dominates a large proportion of Asia, into the Pacific Ocean, which extends from temperate to equatorial latitudes. Altitude range is extreme, spanning from sea-level to more than 8,500 m in the Himalayas, with the average altitude of the Himalayan Tibetan Plateau (HTP) being 4,500 m. This provides the most continental climates on the planet. In contrast, the Pacific Basin is the largest oceanic basin extending from the Arctic in the north to the Southern Ocean (or, depending on definition, to Antarctica) in the south, bounded by Asia and Australia in the west, and the Americas in the east. The climates of small Pacific Islands are the most oceanic in the world. The Asian highland massif contains numerous glaciers. The Himalayan range alone has a total snow and ice cover of 35,110 km^2 containing 3,735 km^3 of permanent snow and ice (Qin et al. 2006).

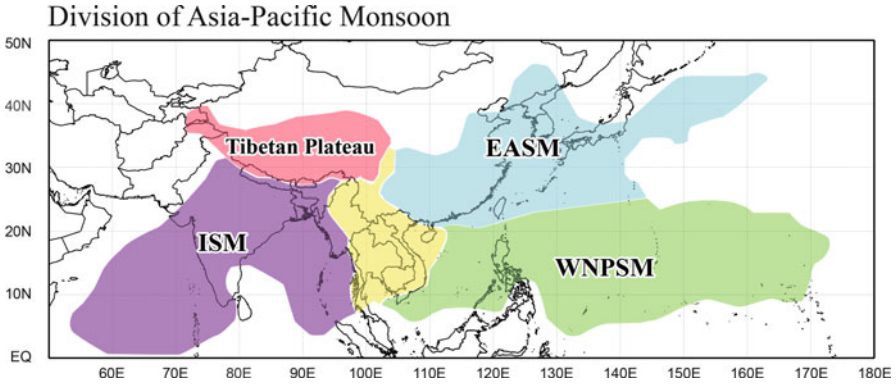

Fig. 2.1 Schematic diagram of the Asian monsoon region: *blue* – the east Asian summer monsoon (*EASM*), *purple* – the Indian summer monsoon (*ISM*), *green* – northwest pacific summer monsoon (*WNPSM*), *yellow* – monsoon buffer, *red* – Qinghai-Tibet Plateau (Reprinted with permission from "Rainy Season of the Asian–Pacific Summer Monsoon," by B. Wang and H. Lin, 2002, Journal of Climate, 15, p. 392. Copyright 2002 by American Meteorological Society. Modified from source)

2.1.2 Large Scale Circulation and the Monsoon System

2.1.2.1 Asia

Monsoon circulation is described as seasonal reversing of wind along with a change of precipitation caused by the asymmetric heating between land and ocean. The Asian monsoon is a most significant component of the global climate system, influencing lifestyles and livelihoods, and providing water resources to nearly 60 % of the world's population. Usually, the summer monsoon season in Asia starts from mid or late May and ends in late September. The Asian monsoon can be classified into some sub-systems, such as south Asian monsoon, east Asian monsoon, south-east Asian monsoon and western north Pacific monsoon (Wang and Lin 2002), but South Asia (India) and East Asia are the two main monsoon areas that have been studied extensively (Fig. 2.1). Besides the strong annual cycle, the Asian monsoon has a wide range of variability from the intra-seasonal, inter-annual to inter-decadal time scales. The intra-seasonal oscillation, with time scales from weeks to months, determines the "active raining period" and "break dry period" of the monsoon, which highlights the importance of intra-seasonal monsoon variability to annual prediction (Webster et al. 1998).

The Asian monsoon is characterized by seasonal migration (northward and withdrawal) of a precipitation belt or the inter-tropical convergence zone (ITCZ) in summer (Gadgil 2003). As shown by Goswami et al. (2006a), the onset of the Indian monsoon starts with a rapid transition of the high precipitation zone from near the equator to about 15°N toward the end of May or beginning of June. Another characteristic is the splitting of the ITCZ into a primary branch over the continental region between 20°N and 25°N, and a secondary branch between the equator and

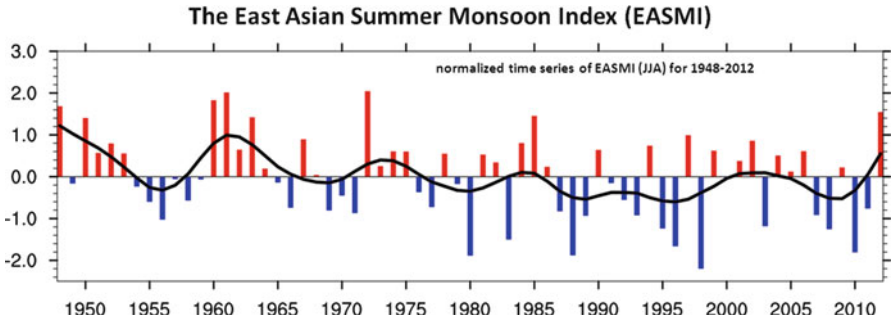

Fig. 2.2 The east Asian summer monsoon index (*EASMI*). Normalized time series (*JJA*) for 1948–2012 (Source: After Li et al. 2010)

10°S. The monsoon tends to withdraw in late September. The northward propagation of the Indian monsoon onset has slowed during the past decade compared with prior decades, and this is consistent with the observed weakening of the May–June mean easterly vertical shear in the region and weakening of the north–south gradient of low-level humidity across the equator. There is evidence to support the hypothesis that the weakening of the easterly shear is due to an eastward shift of the Walker circulation, associated with strengthening of the El Niño phenomenon (Goswami et al. 2010).

The long term trend of the Indian monsoon can be monitored from the observed historical daily precipitation record over India from 1951 to 2001. Goswami et al. (2006a) found rising trends in the frequency and the magnitude of extreme rain events and a significant decreasing trend in the frequency of moderate events over central India during the monsoon seasons. Moreover, a substantial increase in hazards related to heavy rain is expected over central India in the future.

The seasonal migration of the east Asian summer monsoon (EASM) has two stages. The first onset happens in mid-May with the rapid establishment of the Meiyu-Baiu-Changma front. The second onset takes place in early June with the southern ITCZ moving rapidly to about 20°N and establishing dry conditions south of the equator (Goswami et al. 2006a). Many studies have shown weakening of the EASM in recent decades, especially precipitation decreasing from the 1980s in northern China. At the same time, Li et al. (2010) noted a southward shift of the main components of the EASM (the subtropical westerly jet stream, the western Pacific ocean subtropical high, the subtropical Meiyu-Baiu-Changma front, and the tropical monsoon trough) from 1958 to 2008 (Fig. 2.2). Such a southward shift may be due to meridional asymmetries in the regional response to global warming.

The inter-annual variability of the south Asian monsoon and southeast Asian monsoon is strongly related to the El Niño Southern Oscillation (ENSO) phenomenon, with heavy monsoon rainfall in La Niña years and a weak monsoon in El Niño years (for example, Parthasarathy et al. 1994). This interaction is primarily through changes in the equatorial Walker circulation influencing the regional Hadley Circulation (HC) associated with the Asian monsoon (Lau and Nath 2000). Feng

et al. (2011a) show a significant weakening of the northern part of the summer HC and a reverse see-saw relationship of the zonal-mean updraft over 10°N to 20°N and around the equator. This transition is accompanied by the southward retreat of the HC core and is well correlated with the weakening of tropical summer Asian monsoons.

2.1.2.2 Pacific

Surface climates of the tropical Pacific islands are dominated by the vast surrounding ocean and the large-scale atmospheric and oceanic circulations (Streten and Zillman 1984; Terada and Hanzawa 1984). The major atmospheric circulation features include the northeast and southeast trade wind regimes, which originate in the subtropical high pressure belts of each hemisphere where air sinks and dries. These tropical easterly flows are characterized by their constancy in speed and direction, although they tend to be strongest in the respective hemispheric winter season and extend further poleward in the respective hemispheric summer season. The trade winds from the two hemispheres converge in the ITCZ and South Pacific Convergence Zone (SPCZ), where rising air forms the ascending branch of the Hadley Circulation. The HC represents the main north to south component of the Pacific atmospheric circulation. In addition, the Walker Circulation operates in the east to west plane of the tropical Pacific with normally rising air over Indonesia and sinking air in the southeast tropical Pacific. This circulation is intimately linked with the major source of inter-annual tropical climate variability, ENSO.

The SPCZ is one of the most significant features of subtropical southern hemisphere climate (Kiladis et al. 1989; Vincent 1994). It is characterized by low-level convergence of air flow leading to uplift and a band of cloudiness and rainfall stretching from the 'Warm Pool' in the western Pacific south-eastwards towards French Polynesia (Streten and Troup 1973; Kiladis et al. 1989; Vincent 1994). It shares some characteristics with the ITCZ, which lies just north of the Equator, but is more extra tropical in nature, especially east of the Date Line (Trenberth 1976). To the west, it is linked to the ITCZ over the Warm Pool. To the east, it is maintained by the interaction of the trade winds and transient disturbances in the mid-latitude westerly winds propagating from the Australasian region. It tends to lie over a region of large sea surface temperature (SST) gradient, rather than the maximum of SST, and is most active in the Austral (southern hemisphere) summer period (November-April). The location of the convergence maximum of the SPCZ shows considerable variability between seasons, varying by 10–15° of latitude. This causes large variability in rainfall throughout the southwest Pacific.

The Pacific North American (PNA) oscillation (Wallace and Gutzler 1981) describes large-scale features over the North Pacific Ocean and the North American continent, and it has a significant influence on the weather of the Pacific. In its positive phase, the PNA is associated with enhanced ridging of the pressure over western North America and deeper troughs over the central north Pacific and southeastern USA. Variations in the PNA oscillation on time scales of days to

months can be predicted with some skill (Johansson 2007), and there is some evidence of links between the PNA oscillation pattern and variations in the large-scale ENSO (Straus and Shukla 2002).

2.1.3 Drivers of Climate Variability and Trends Across Asia-Pacific

Superimposed on the average seasonal cycles of surface climate and observed trends in Asia-Pacific surface climate are various sources of natural climate variability that modulate atmospheric and oceanic climate on time scales from weeks to decades.

2.1.3.1 El Niño-Southern Oscillation (ENSO)

The ENSO phenomenon is the principle source of inter-annual global climate variability. This highly coupled ocean–atmosphere phenomenon is centered in the tropical Pacific. ENSO has significant climate and societal impacts both within the region and, through teleconnections (Fig. 2.3), to many distant parts of the world (Troup 1965; Trenberth 1991, 1997; McPhaden et al. 2006; Trenberth et al. 2007). ENSO fluctuates between two phases, which change the normal Asia-Pacific atmospheric and oceanic circulations. During El Niño events, the easterly trade winds weaken along the equatorial Pacific and a large part of the equatorial Pacific experiences unusually warm SSTs, and warmer than normal SSTs in a large part of the Indian Ocean and warmer than normal surface temperatures over south and south east Asia. At the same time, SSTs are cooler than normal in the subtropical southwest and northwest Pacific and Papua-New Guinea. This is associated with a weakening of the horizontal Walker Circulation and strengthening of the meridional HC. The centre of intense tropical convection shifts eastward towards the Date Line and the ITCZ and SPCZ move closer to the equator. As a result, precipitation is higher than normal in the equatorial Pacific, but lower than normal over South and Southeast Asia, Indonesia, eastern Australia, and the Southwest Pacific with some regions experiencing drought conditions. There are also shifts in the preferred location of tropical cyclone activity. The slope of the thermocline (separating warmer surface and cooler deeper waters) flattens across the Pacific Ocean, and the Warm Pool shifts eastwards.

Fig. 2.3 (continued) for 1958–2004, and GPCP precipitation for 1979–2003 (*bottom left*), updated from Trenberth and Caron (2000). The Darwin-based SOI, in normalized units of standard deviation, from 1866 to 2005 (Können et al. 1988; *lower right*) features monthly values with an 11-point low-pass filter, which effectively removes fluctuations with periods of less than 8 months (Trenberth 1984). The smooth *black* curve shows decadal variations. *Red* values indicate positive sea level pressure anomalies at Darwin and thus El Niño conditions (Source: Trenberth et al. 2007) (Reprinted with permission from "Climate Change 2007: The Physical Science Basis. Working Group I Contribution to the Fourth Assessment Report of the Intergovernmental Panel on Climate Change," Cambridge University Press, Figure 3.27, p. 288)

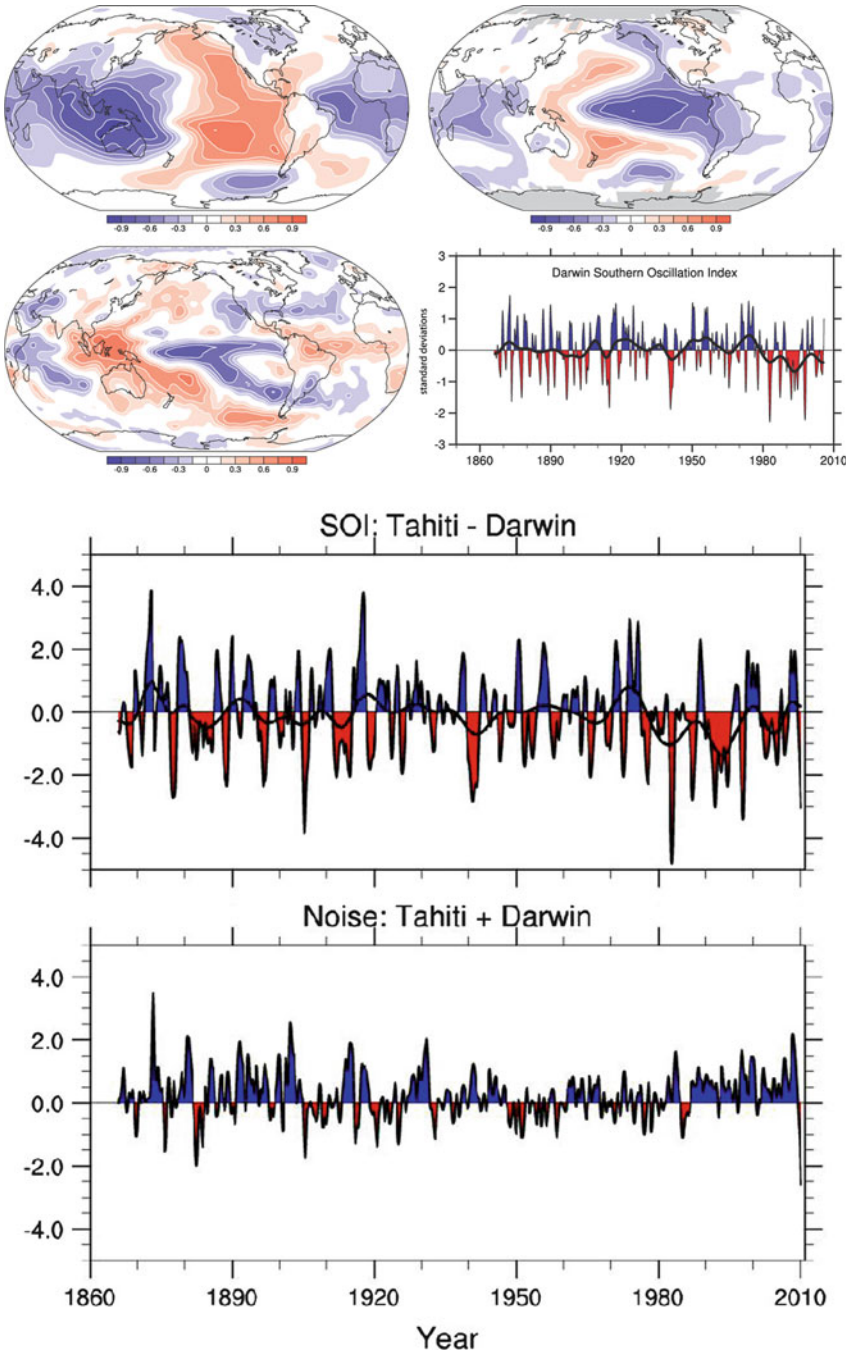

Fig. 2.3 Correlations with the SOI, based on normalised Tahiti minus Darwin sea level pressures, for annual (May to April) means for sea level pressure (*top left*) and surface temperature (*top right*)

Climate anomalies during La Niña events are typically opposite to those of El Niño events, with stronger trade winds and large parts of the Pacific, as well as the Indian Ocean and south Asia, experiencing cooler than normal SSTs. Higher than normal temperatures and SSTs occur in the southwest and northwest Pacific. There are changes in the usual locations of tropical cyclones and a shift of the heaviest rainfall zone to the far western tropical Pacific, East Australia, Indonesia and South and Southeast Asia. The depth of the thermocline also increases from east to west across the Pacific for La Niña; this difference is reduced during El Niño.

Both phases of ENSO typically evolve over a period of 12–18 months and have some predictability once they have started to develop. Seasonal outlooks of ENSO conditions have improved significantly in reliability and are based on being able to successfully observe and model the development of SST anomalies in the tropical Pacific up to a year in advance of an event (McPhaden 2004). Two commonly used indices of ENSO activity are (1) the Southern Oscillation Index (SOI), which measures the atmospheric component and represents the anomalous sea level pressure difference between Tahiti in the southwest Pacific and Darwin in northern Australia, and (2) the Niño 3.4 region (5°N to 5°S, 170°W to 120°W) average SST anomaly, which captures the oceanic component of ENSO. These indices are very similar, indicating the highly-coupled ocean–atmosphere nature of ENSO but also show differences in the timing and magnitude of individual events, which typically recur every 3–7 years.

Although each ENSO event evolves slightly differently, there are common features to these different 'flavours' (Trenberth and Stepaniak 2001) and features typical of the two phases can be determined by averaging the surface climate anomalies across several events. The traditional El Niño, also called Eastern Pacific (EP) El Niño, involves temperature anomalies in the eastern Pacific. However, in the last two decades of the twentieth century non-traditional El Niño patterns are observed, in which the usual place of the temperature anomaly (Niño 1 and 2) is not affected, but an anomaly arises in the central Pacific (Niño 3.4). The phenomenon is called Central Pacific (CP) El Niño, "Date Line" El Niño or El Niño "Modoki" (Larkin and Harrison 2005). Depending on the season, the impacts over regions such as East Asia, New Zealand, and the western coast of USA can be different from those of the traditional ENSO.

ENSO events also affect the spatial occurrence of tropical cyclone activity in the southwest Pacific. During El Niño episodes, the overall number of tropical cyclones tends to be lower, with highest occurrences between Vanuatu and Fiji, and chances of occurrence higher further east in Samoa, southern Cook Islands and French Polynesia. During La Niña events, tropical cyclones are more frequent in the Coral Sea, with highest occurrence around New Caledonia, and higher occurrence between the coast of Queensland and Vanuatu. During these seasons, there is an absence of tropical cyclones from the Cook Islands eastwards. The location of the SPCZ also varies systematically with ENSO-related expansion and contraction of the Warm Pool (Folland et al. 2002). Such movements can result in very large precipitation anomalies on either side of the mean location of the SPCZ (Salinger et al. 1995), as it moves northeast during El Niño events and southwest during La Niña events.

A recent modeling study simulated the effects of climate change on ENSO over the twenty-first century. The study found no significant changes in its extent or frequency, but the warmer and moister atmosphere of the future could make ENSO events more extreme (Stevenson et al. 2011). However, there remains considerable uncertainty in the future behavior of ENSO under climate change conditions.

2.1.3.2 Indian Ocean Dipole

ENSO is found to be associated with inter-annual variability of the Indian summer monsoon (for example, Webster et al. 1998), but this relationship may be weakening in recent decades (Kinter et al. 2002). The linkage between the Indian monsoon and Indian Ocean Dipole (IOD) has been the subject of many investigations, such as Saji et al. (1999) and Webster et al. (1999). The IOD manifests through an east–west gradient of tropical SST, which in one extreme phase in boreal autumn shows cooling and drying off Sumatra and warming off Somalia in the west, combined with anomalous easterlies along the Equator. In a negative dipole year, the reverse occurs, with Indonesia much warmer and wetter. Several recent IOD events have occurred simultaneously with ENSO events. The strongest IOD episode ever observed occurred in 1997–1998. Trenberth et al. (2002) showed that Indian Ocean SSTs tend to rise about 5 months after the peak of ENSO in the Pacific. Monsoon variability (Lau and Nath 2004) is also likely to play a role in triggering or intensifying IOD events. Decadal variability in correlations between SST-based indices of the IOD and ENSO has been documented (Clark et al. 2003). At interdecadal time scales, the SST patterns associated with the variability of ENSO indices are very similar to the SST patterns associated with the Indian monsoon rainfall (Krishnamurthy and Goswami 2000) and with the North Pacific inter-decadal variability (Deser et al. 2004), raising the issue of coupled mechanisms modulating both ENSO-monsoon system and IOD variability (Terray et al. 2005). It has been shown that a positive IOD index can reduce the effect of ENSO, resulting in increased monsoon rains in some ENSO years such as 1983, 1994 and 1997. Further, it has been shown that the two poles of the IOD – the eastern pole (around Indonesia) and the western pole (off the African coast) – can independently and cumulatively affect the rainfall for the monsoon in the Indian subcontinent.

2.1.3.3 Pacific Decadal Oscillation (PDO)/Interdecadal Pacific Oscillation (IPO)

The inter-annual variability of ENSO and the strength of its climate teleconnections are modulated on decadal time scales by a long-lived pattern of Pacific climate variability known as the Pacific Decadal Oscillation (PDO) (Mantua et al. 1997; Zhang et al. 1997) or the Interdecadal Pacific Oscillation (IPO) (Power et al. 1999). The PDO is the North Pacific part of a Pacific basin-wide pattern encompassed by the IPO and is described by an "El Niño-like" pattern of Pacific SST anomalies and appears to persist in either a warm or cool phase for several decades (Fig. 2.4). Warm phases

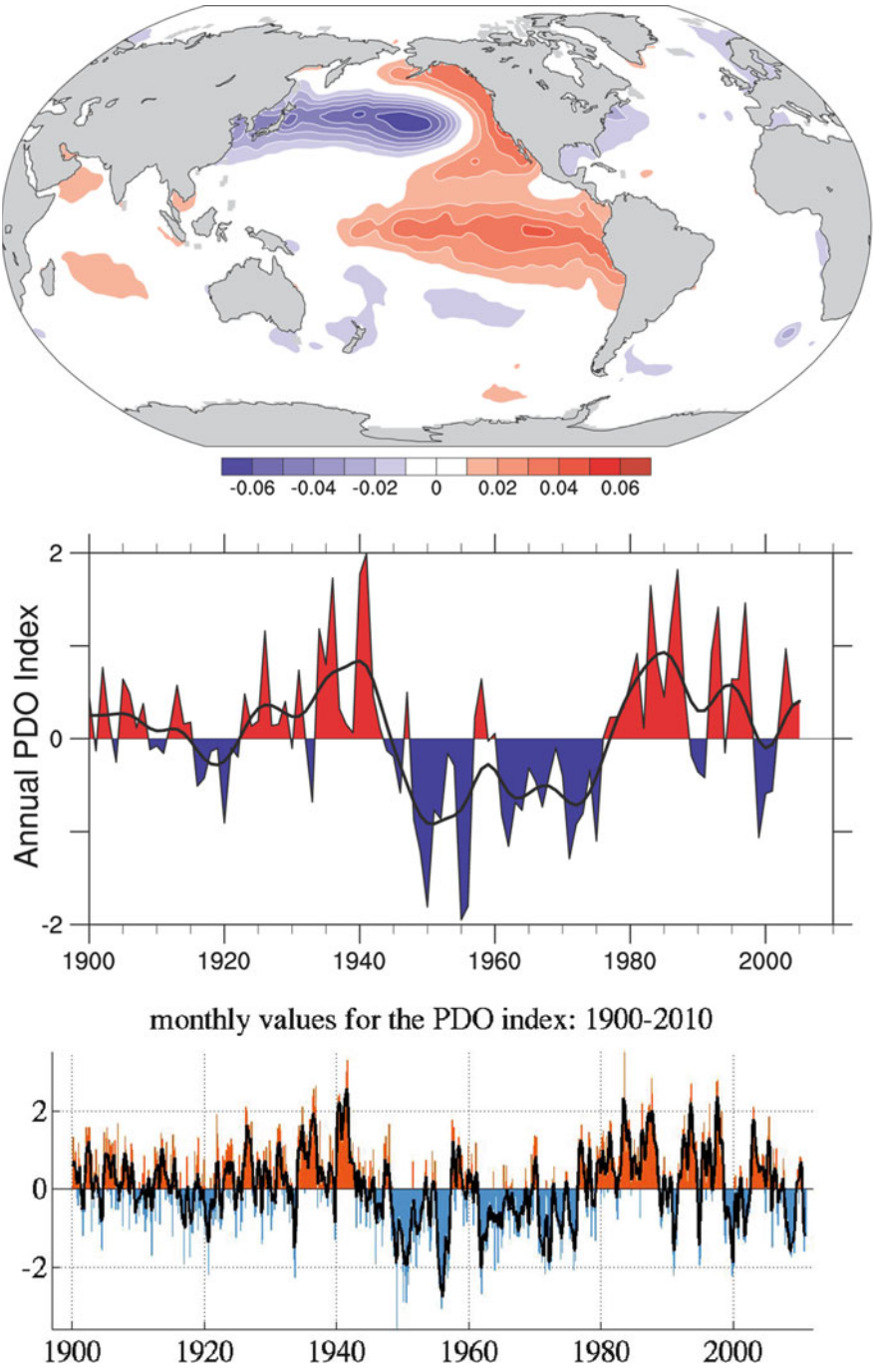

Fig. 2.4 Pacific Decadal Oscillation: (*top*) SST based on the leading EOF SST pattern for the Pacific basin north of 20°N for 1901–2004 (updated; see Mantua et al. 1997; Power et al. 1999) and projected for the global ocean (units are non-dimensional); and (*bottom*) annual time series (Updated from Mantua et al. 1997) (Reprinted with permission from "Climate Change 2007: The Physical Science Basis. Working Group I Contribution to the Fourth Assessment Report of the Intergovernmental Panel on Climate Change," Cambridge University Press, Figure 3.28, p. 289)

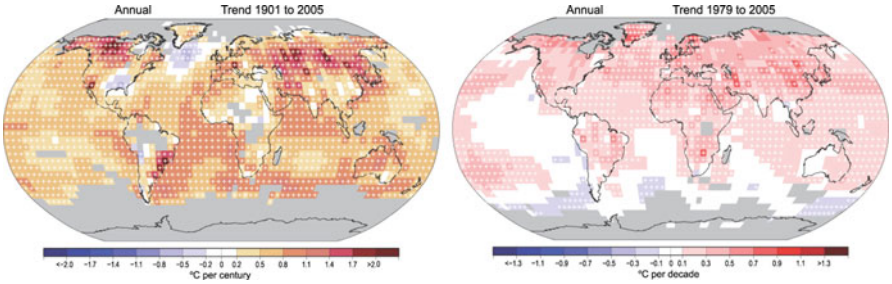

Fig. 2.5 Linear trend of annual temperatures for 1901–2005 (*left*; °C per century) and 1979–2005 (*right*; °C per decade). Areas in *grey* have insufficient data to produce reliable trends. The minimum number of years needed to calculate a trend value is 66 years for 1901–2005 and 18 years for 1979–2005. An annual value is available if there are 10 valid monthly temperature anomaly values. The data set used was produced by NCDC from Smith and Reynolds (2005). Trends significant at the 5 % level are indicated by *white + marks* (Reprinted with permission from "Climate Change 2007: The Physical Science Basis. Working Group I Contribution to the Fourth Assessment Report of the Intergovernmental Panel on Climate Change," Cambridge University Press, Figure 3.9, p. 250)

characterized the 1920s–1940s and from the mid-1970s to the late 1990s. In these periods, ENSO was a weaker source of inter-annual climate variability. The warm phases were preceded and separated by IPO and PDO cool phases from the 1900s to 1920s and 1940s to 1970s, when ENSO was a major source of inter-annual climate variability (Deser et al. 2004). Decadal variability in the SST field of the Pacific is associated with decadal variability in atmospheric variables, such as sea-level pressure, winds and precipitation (Deser et al. 2004; Burgman et al. 2008). The nature of ENSO has varied considerably over time. The 1976–1977 PDO/IPO climate shift (Trenberth 1990) was associated with marked changes in El Niño evolution (Trenberth and Stepaniak 2001), a shift to generally above-normal SSTs in the eastern and central equatorial Pacific and a tendency towards more prolonged and stronger El Niños. This tendency reversed in 1998/1999 with the latest negative phase of the PDO.

2.1.4 Trends and Extremes

2.1.4.1 Surface Temperature and Precipitation

Warming in mean surface air temperature over the period 1901–2005 (Fig. 2.5) range from as high as 1.5 °C over Siberia, and at least 1.0 °C/century over northern Asia (Trenberth et al. 2007). Over the remainder of the Asian continent the rate has been 0.8–1.0 °C/century as well as in northern Australia. This compares with a warming rate of 0.5–0.8 °C/century for the Pacific and remainder of Oceania. Higher latitude regions in Asia are experiencing a faster rate of warming than temperate regions. For example, winter temperatures in Mongolia have increased on average by 3.6 °C over the past 60 years (Bohannon 2008). A number of Asian countries have found that winter temperatures are changing faster than summer, and that heat waves are lasting longer (Cruz et al. 2007).

For the period 1979–2005 the warming trend per decade reflects a similar pattern with rates in excess of 0.5 °C/decade over much of the entire Asian continent. In South Asia and Oceania warming rates are between 0.1 °C and 0.3 °C/decade, with the least warming in the tropical and eastern Pacific Ocean (0.1 °C/decade).

Land-based records of accurate trends in precipitation for the Asia-Pacific region can only be gleaned from a much sparser network of observing stations. For the period 1901–2005 (Fig. 2.6) most stations over Asia and Australia record a precipitation increase of between 20 % and 40 % per century. Increases from 10 % to 30 % per decade have occurred over northwest Asia and northwest Australia, western New Zealand and parts of the western tropical Pacific. Over India, eastern precipitation has decreased from 5 % to 15 % per decade (Trenberth et al. 2007).

Over much of Asia the regional climate has been affected not only by the effects of enhanced levels of greenhouse gases (GHGs), but also by high levels of aerosols produced mainly from biomass burning and the consumption of fossil fuels (Ramanathan et al. 2007). The resulting atmospheric brown cloud (ABC) affects the radiation budget of the atmosphere (through both the scattering and absorption of radiation) and the properties of clouds. There is both observational and modeling evidence of ABC impacts on both temperature and precipitation in Asia (Nakajima et al. 2007). There is considerable evidence (Wild 2009a) that the scattering effect of aerosols reduced solar radiation reaching the surface ('global dimming') for some decades in the last half of the twentieth century, and hence masked some of the warming effects of enhanced levels of GHGs. While this dimming effect has been reduced in some parts of the world over the last decade or so, there has been a continuing decline in surface solar radiation in China and India (Wild et al. 2009).

2.1.4.2 Tropical Cyclones

At the global level there are no clear trends in the intensity and frequency of tropical cyclones over the last half of the twentieth century (Knutson et al. 2010). However, there are some indications of trends at the regional level. For Asia and the Pacific there is evidence of increases in the intensity and frequency of tropical cyclones as well as intense rainfall, tornadoes and thunderstorms (Cruz et al. 2007). Analysis of Pacific Ocean extra-tropical cyclones over the past 50 years suggests that, while the overall frequency of storms has not changed, the frequency of intense storms has increased. Moreover, both observational studies and modeling projections indicate that the intensity of cyclones in the North Pacific is increasing (Lambert and Fyfe 2006).

2.1.4.3 Glaciers

(a) *Glacier mass balance studies*
There have been few field studies on glaciers in Asia, and there is not a clear picture of how the region is expected to change in the coming decades. The main

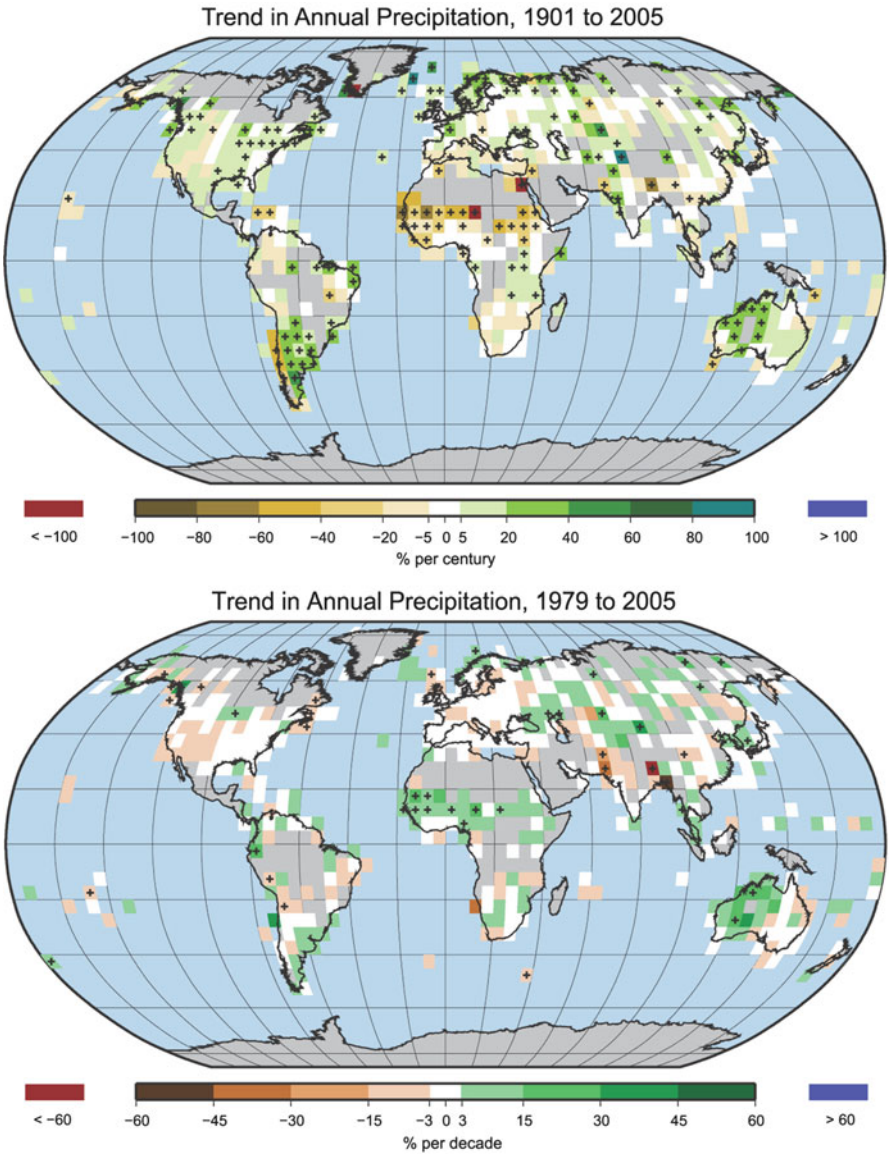

Fig. 2.6 Trend of annual land precipitation amounts for 1901–2005 (*top*, % per century) and 1979–2005 (*bottom*, % per decade), using the GHCN precipitation data set from NCDC. The percentage is based on the means for the 1961–1990 period. Areas in *grey* have insufficient data to produce reliable trends. The minimum number of years required to calculate a trend value is 66 for 1901–2005 and 18 for 1979–2005. An annual value is complete for a given year if all 12 monthly percentage anomaly values are present. Note the different colour bars and units in each plot. Trends significant at the 5 % level are indicated by *black + marks* (Reprinted with permission from "Climate Change 2007: The Physical Science Basis. Working Group I Contribution to the Fourth Assessment Report of the Intergovernmental Panel on Climate Change," Cambridge University Press, Figure 3.13, p. 256)

difficulty is the accessibility of glaciers because of the steep topography with rugged terrain. Moreover, large costs are incurred in carrying out studies in such hard-to-reach places. Assessment of mass balance of the glaciers of the region has been carried out by evaluating each succeeding year's glacier surface vis-à-vis its position in the previous year, or by evaluating the respective glacier surface at the end of the accumulation and ablation season. From these trends the glacier mass balance can be evaluated.

Since the glacier inventory work carried out by Muller (1970) in the Mount Everest region, Glaciological Expedition to Nepal (GEN), a Nepal-Japan joint venture, undertook the task of making a glacier inventory of Nepal early in the 1970s (Higuchi et al. 1976; Watanabe 1976). Most of the works were carried out with the help of aircraft observations and ground field surveys. The advancement of remote sensing technology facilitated this survey work of making an inventory of glaciers in other parts of the Himalaya-Tibetan Plateau (HTP) region. The Hindu Kush-Himalaya (HKH) is an extensive area, which alone contains more than 15,000 glaciers and snow fields (Ives et al. 2010).

(b) *Field studies*

In order to understand the dynamics of glaciers, field studies become an important activity and some examples are presented from the Asia and Pacific region.

Nepal

The Nepal Himalayas contain around 3,252 glaciers. Field studies are constrained by the rugged terrain and remoteness. However, some studies have been carried out in the central and eastern Himalaya regions of Nepal. The mass balance studies of the glaciers were carried out in Hidden Valley located in the northern side of the central Himalaya during the monsoon season of 1974 (Nakawo et al. 1976; Fujii et al. 1976) and such activities are beginning in Nepal. There have been few studies of the glaciers on the northern side of the Nepal Himalayas; Watanabe et al. (1967) is an exception. The Hidden Valley work therefore has special significance. Among the studied glaciers in the Hidden Valley, Rikha Samba glacier is the largest with an area of 4.81 km^2 and an altitude span from 5,245 to 5,985 m. For the glaciers of Nepal, accumulation and ablation occur mainly in the boreal summer. Although the Hidden Valley is situated on the northern side of the Himalayas with low precipitation totals, it is still influenced by the Asia monsoon (Shrestha et al. 1976). Glaciers in the Hidden Valley have shown considerable retreat during the period 1974–1994 (Fujii et al. 1996).

Figure 2.7 shows the evolution of the Rikha Samba Glacier from 1974 to 2010. It clearly shows the depletion of the snout of the glacier. The rate at which Himalayan glaciers are shrinking generally remains poorly constrained because ground-based observations are limited by the high altitude and remoteness of the region.

Fujita and Nuimura (2011) looked at the mass wastage of the Himalayan glaciers and they selected three benchmark glaciers in the Nepal Himalayas on which observations have been made since the 1970s. Based on in situ measurements,

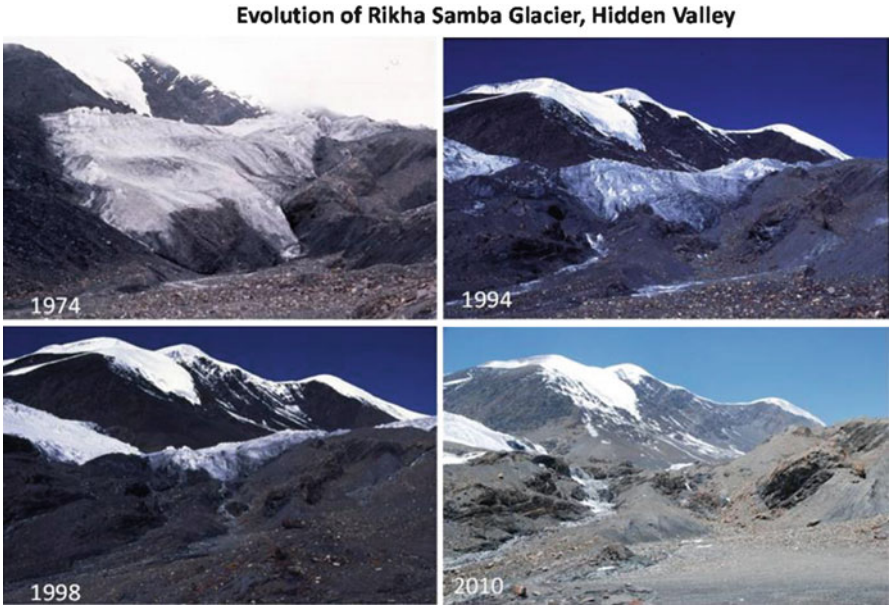

Fig. 2.7 Time sequence of Rikha Samba glacier, Hidden Valley (Source: Madan L. Shrestha, Koji Fujita, Glaciological Expedition of Nepal (*GEN*), and Department of Hydrology and Meteorology (*DHM*) Nepal)

the wastage rate of the glaciers is equivalent to the global mean during the recent decade (2000–2010), but is higher than the global mean during the previous two decades. This study also indicates that some glaciers at lower altitudes may disappear sooner than those at higher altitudes (Fig. 2.8). However, the heterogeneous distribution of the Equilibrium Line Altitudes (ELAs) trends suggest that it is unwarranted to draw conclusions regarding the fate of the Himalayan glaciers based on such a small number of examples, especially when the benchmark glaciers are chosen partly because of their small size, small elevation range, and simple geometry. In addition, other variables like nature, intensity and quantity of precipitation along with temperature, cloud cover, wind and radiation play an important role and respond in a complex manner through their impact on glacier fluctuations.

India

In the India Himalayas, all available sources illustrate that almost all the glaciers are in a state of depletion. As an example, the Gangotri glacier has been in a continuous state of retreat and fragmentation during the past century. The length of the glacier has been computed for different years based on available data, showing that the length of the glacier has reduced by about 0.59 km in 33 years, from 1976 to 2009, with an average retreat rate of 17.59 m/year. The analysis shows that the glacier is not only receding in length but also in terms of

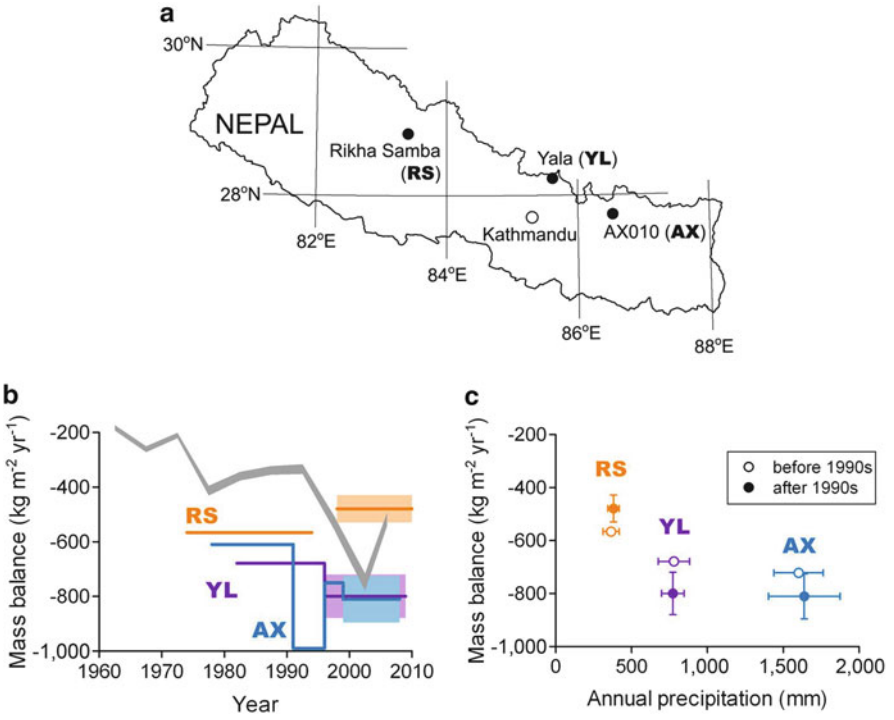

Fig. 2.8 Location of the three benchmark glaciers in Nepal (**a**), temporal changes in the area-averaged mass balances of the glaciers compared with the pentadal global mean (*grey line*) (Cogley et al. 2010) (**b**), and mass balances compared with annual precipitation (**c**). *Colour* shading in **b** and *vertical* bars in **c** denote measurement errors of mass balance. *Horizontal* bars in **c** denote variability of annual precipitation (Source: Fujita and Nuimura 2011) (Reprinted from "Spatially heterogeneous wastage of Himalayan glaciers," by K. Fujita and T. Nuimura, 2011, PNAS, 108(34), Figure 1, p. 2)

glaciated area from all sides. Analysis shows that between 1976 and 2006, the glacier area has reduced by 15.5 km^2, with an average loss of 0.51 km^2 per year. With a reduction in the area and length of the Gangotri glacier, there has also been a retreat in the snout position. Similar reductions have also been observed in most of the other glaciers (Kumar et al. 2009) indicating a significant change in the glaciers in the India Himalayas.

New Zealand

There are few places in the Pacific region with glaciers. New Zealand has glaciers with a long, continuous record of annual end-of-summer-snowline measurements for a set of Southern Alps 'index glaciers' from 1977 to present. Chinn et al. (2012) used these index glaciers to estimate annual mass balance and volume water equivalent changes to the over 3,000 glaciers on the Southern Alps. Results show that estimated ice volume in water equivalents for the Southern Alps has decreased from 54.5 km^3 in 1976 to 46.1 km^3 by 2008. This

equates to a loss rate of 0.3 km^3a^{-1} over the last three decades, but this is considerably less than the rate of ice volume loss estimated for the previous 100 years. Results show that there are significant correlations with an index of southwest/northeast circulation over New Zealand in the ablation season. El Niño years are associated with mass balance gains and La Niña years with mass balance losses. There are also significant correlations with the Southern Annular Mode, also known as the Antarctic Oscillation (Kidson 1999).

2.1.4.4 Extreme Events

Manton et al. (2001) and Kwon (2007) analyzed trends in climate extremes in the Asia-Pacific region using 20 extreme temperature indices and 10 extreme precipitation indices classified into three groups: percentile-based indices, fixed-threshold-based indices, and others. Percentile-based extreme temperature indices include cool/warm nights/days (upper and lower 10th percentiles). Similarly, percentile-based extreme precipitation indices include very wet days (95th percentile). Other indices included the number of consecutive dry/wet days. Thirty-year (1971–2000) average values were used to calculate each extreme index from daily maximum/minimum or precipitation data at individual weather stations. A linear regression was fitted to the time series of extreme climate indices for each weather station over the period 1955–2007, and significant levels of the slope values are calculated using the RClimDex software (Zhang and Yang 2004).

Figures 2.9, 2.10 and 2.11 show spatial patterns of linear trends of extreme climate indices over the period 1955–2007 across the region. Among the fifth upper or lower percentile-based indices including cool/warm days/nights, the magnitude of changes in cool nights are greatest at both low- and mid-latitude regions. As shown in Fig. 2.9, cool nights have decreased most in Southeast Asia at the rate of 20 days/decade or more. In the mid-latitude regions above 30°N, cool nights have decreased at the rate of 0–10 days/decade. In central Australia, the trends are not statistically significant and also show reversed signs.

The magnitude of trends in cool days lies within the range of 0–10 days/decade in most of the Asia-Pacific land areas (Fig. 2.10). In India (Kothawale et al. 2009) the frequency of hot days and warm nights shows a widespread increase from 1970 to 2005, especially over southern India. Cool days and cold nights have a widespread decrease. Trends in Nepal (Baidya et al. 2008) show an increase in hot days and warm nights. Most of the temperature extreme indices show a consistently different pattern in the mountainous and southern plains of Nepal (Terai belt). The trend has relatively higher magnitude in mountainous regions where permanent snow and glaciers occur.

Frost days do not occur in the tropical regions between 30°N and 30°S. Regions where frost days do not occur extend more southward in the Southern Hemisphere compared with the northern limit of no frost days. For instance, the southern limit of no frost days occurs in New Zealand (mid-latitude), while the northern limit is located in southern China (subtropical region). In many regions in the mid-latitude

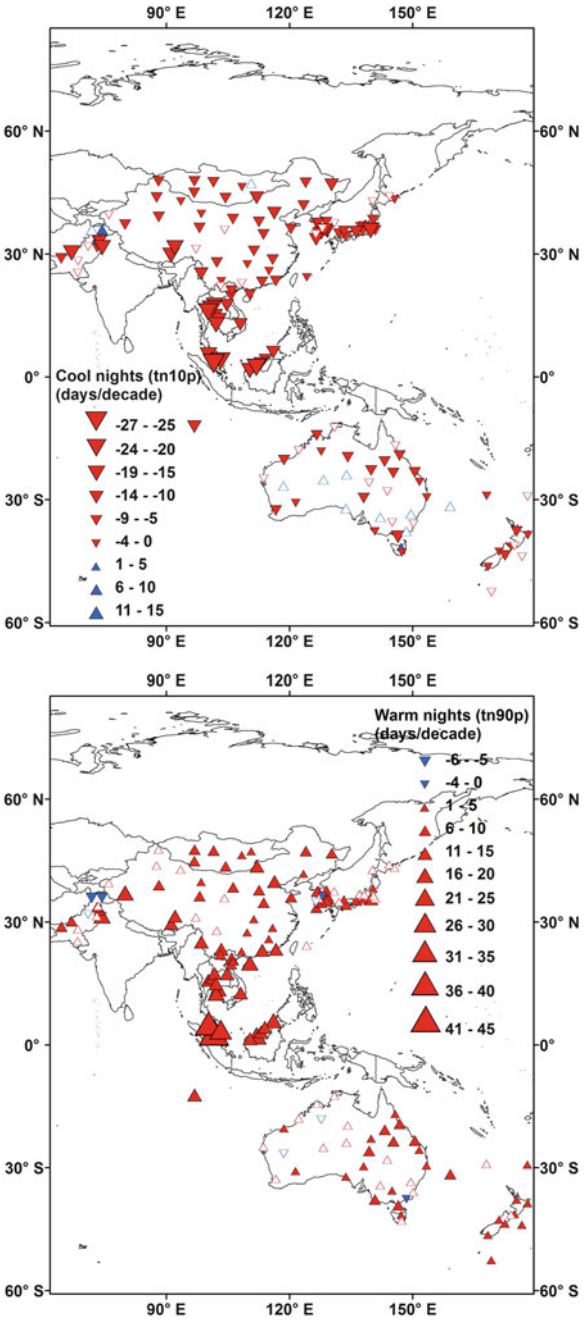

Fig. 2.9 Trends (days/decade) in the frequency of warm (*tn90p*) and cool (*tn10p*) nights over the period 1955–2007 across ten Asia-Pacific countries; *colour-filled symbols* indicate trend is significant at 95 % level; the frequency of cool nights is decreasing across the region (Source: Kwon 2007)

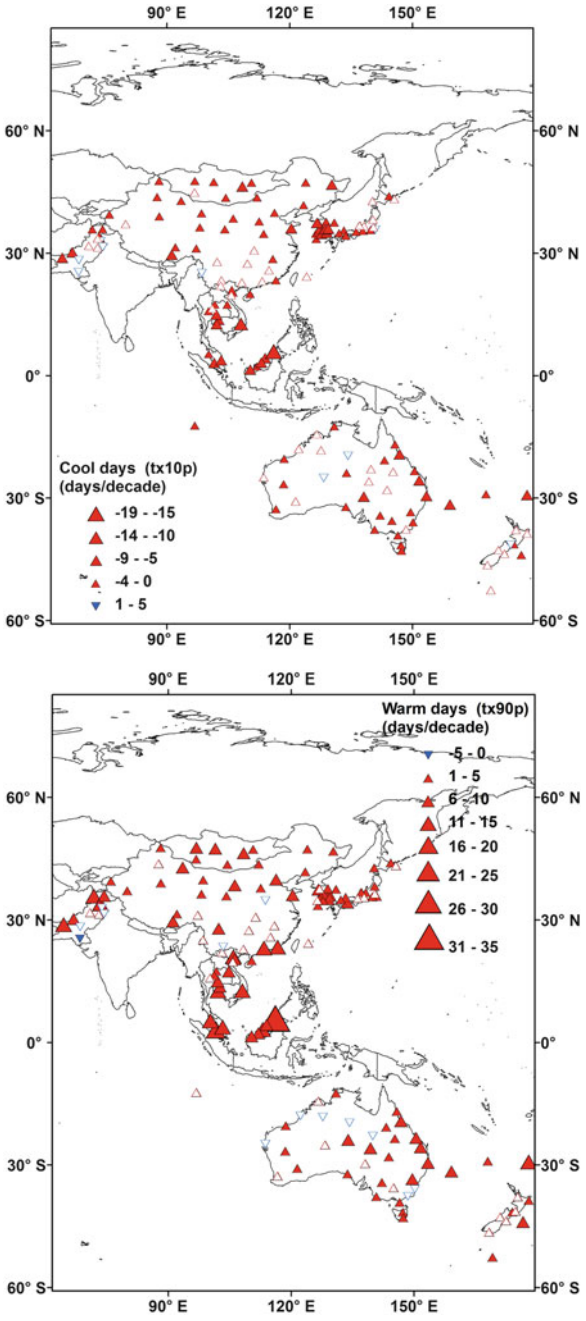

Fig. 2.10 Trends (days/decade) in the frequency of cool (*tx10p*) and warm (*tx90p*) days over the period 1955–2007 across ten Asia-Pacific countries; *colour-filled symbols* indicate trend is significant at 95 % level; the frequency of cool nights is decreasing across the region (Source: Kwon 2007)

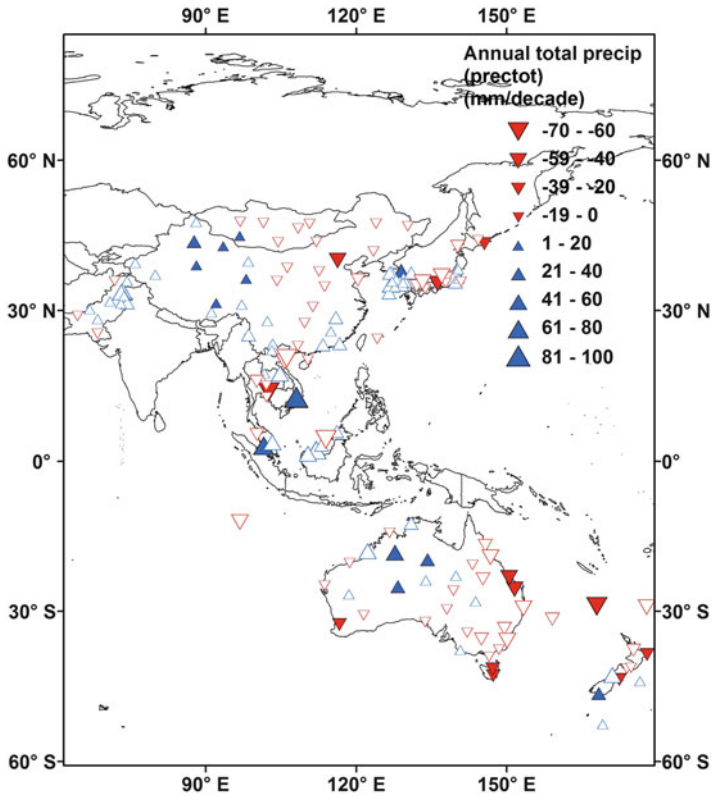

Fig. 2.11 Linear trends (mm/decade) of annual total precipitation day amount (*prcptot*) over the 1955–2007 period across ten across ten Asia-Pacific countries. *Colour-filled symbols* indicate that the linear trend is significance at the 95 % level (Source: Kwon 2007)

of the Southern Hemisphere, frost days are relatively rare. In contrast, over the continents including China and Mongolia, the number of frost days has decreased in the range of 0–8 days/decade. Compared with frost days, significant trends of summer days are observed in both 50°N and 40°S.

Spatial patterns of linear trends of annual total precipitation amount (prcptot) are illustrated in Fig. 2.11. Overall, the trends vary from one location to another. It is difficult to identify regionally-coherent significant trends. However, if insignificant trends are also considered, the overall decreasing trends of annual total precipitation amount are observed in northern China and south eastern Australia, while the increasing trends are found in the Tibetan plateau, Southeast Asia, Republic of Korea and north-western Australia, implying that the summer monsoon system may be intensified in these regions.

As shown in Fig. 2.12, similar patterns are observed for trends in very wet days. For India (Joshi and Rajeevan 2006), for the period 1901–2000, positive trends are seen over the west coast and north western parts of the Indian peninsula. In contrast

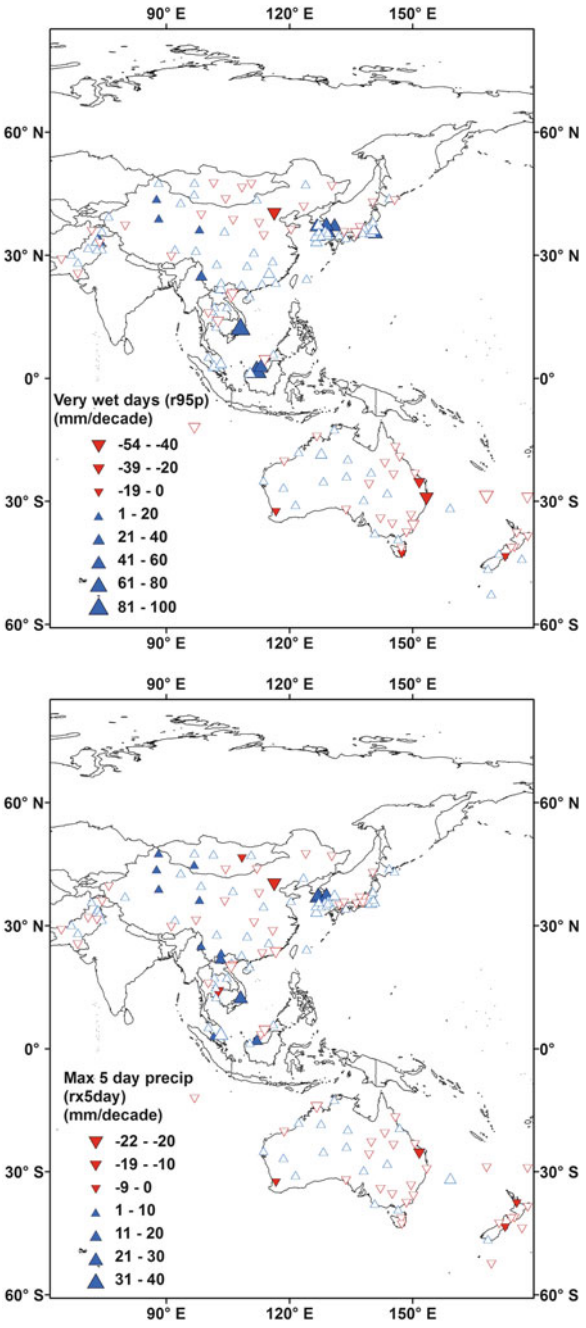

Fig. 2.12 Trends for very wet days (*r95p*) and consecutive dry days (*cdd*) over the 1955–2007 period across ten Asia-Pacific countries. *Colour-filled symbols* indicate that the linear trend is significant at the 95 % level (Source: Kwon 2007)

to extreme rainfall events, a decrease is seen in the frequency of moderate rainfall events over central India during the monsoon season from 1950 to 2000 (Goswami et al. 2006b). Strong increasing trends of the very wet day index are observed in Southeast Asia and Republic of Korea, where heavy rainfall events occur during the monsoon period. In contrast, there are decreasing trends in northern China and south-eastern Australia. There is no noticeable regionally-coherent pattern in trends in consecutive dry days. The magnitude and sign of the trends vary substantially from place to place.

Recently, Liu et al. (2009) obtained some interesting results through a series of analyses on how the intensity of precipitation reacts to global warming. Starting with observations from Taiwan, they found that the 90th percentile of precipitation intensity increases by about 95 % for each degree C increase in global mean temperature; the global average precipitation intensity increases by about 23 % per degree C. Their study clearly showed the linkage between increasing extreme events and global warming.

2.1.5 Attribution of Change

IPCC (2007b) notes that anthropogenic change has been detected in global surface temperature with very high significance levels (at least the 1 % level). This conclusion is strengthened by the detection of changes in the upper ocean with high significance level. Upper ocean warming argues against the surface warming being due to natural internal processes. The observed change is very large relative to climate model-simulated internal variability. Surface temperature variability simulated by models is consistent with the variability estimated from the instrumental record. These conclusions apply to observed temperature change over Asia and the Pacific.

It can also be concluded that anthropogenic forcing has contributed to widespread glacier retreat during the twentieth century in Central Asia, the Himalayan plateau and the Southern Alps of New Zealand.

A range of observational evidence indicates that temperature extremes are changing. An anthropogenic influence on warm and cold nights is consistent with that expected from global warming, as is the increase in high intensity rainfall events. The detection of changes in temperature extremes is supported by other comparisons between models and observations. Model uncertainties in changes in temperature extremes are greater than for mean temperatures and there is limited observational coverage and substantial observational uncertainty (IPCC 2012).

The current understanding of climate change in the monsoon regions remains considerably uncertain with respect to circulation and precipitation. IPCC (2007a) records that the Asian monsoon circulation is likely to decrease by 15 % by the late twenty-first century under the SRES A1B scenario (Tanaka et al. 2005). These results are consistent with simulations (Ramanathan et al. 2005; Tanaka et al. 2005) of weakening monsoons due to anthropogenic factors, but further model and empirical studies are required to confirm this.

Observations indicate that the HC has widened by about 2–5° since 1979 (Johanson and Fu 2009). This widening and the concomitant poleward displacement of the subtropical dry zones may be accompanied by large-scale drying near 30°N and 30°S. Simple and comprehensive global climate models (GCMs) indicate that the HC may widen in response to global warming, warming of the western Pacific, or polar stratospheric cooling. Observational and modeling evidence has been found of changes in the HC affecting the rainfall of south eastern Australia (Lucas et al. 2012; Timbal and Drosdowsky 2012). The observed HC widening cannot be explained by natural variability alone, and it is also significantly larger than in simulations of the twentieth and twenty-first centuries (Kent et al. 2011). These results illustrate the need for further investigation into the nature and causes of the widening of the HC.

2.2 Modeling Projections and Regional Downscaling

2.2.1 Introduction

Climate modeling over the Asian region involves some significant complexities. The topography of the region includes many small islands with extensive coastlines, producing many complicated sea-breeze and land-breeze effects. There is also much significant orography, including the Himalayas and Tibetan plateau where there are extra effects from snow and snow melt. Monsoon behavior in the region is still difficult to capture well in global climate models (GCMs); this is partly due to a lack of horizontal resolution in GCMs, and so various topographic interactions with the atmospheric flow are not adequately captured. The complex topography also affects the ability to properly represent relevant physical processes within the models. A particular problem occurs with handling moist convective processes, which require complex diurnally-varying triggering of the convection, and an associated detailed treatment of the atmospheric boundary layer, in order to adequately represent the sea- and land-breeze effects.

As a result, there is a requirement for quite fine resolution over the Asian region to resolve the complex topographic features. One approach, called dynamical downscaling, is to use high-resolution models formulated with the same dynamical equations of motion as the GCMs, driven in some manner by the GCM simulations, which typically have a horizontal resolution of 100–200 km. The dynamical downscaling technique has been available for about 20 years, and the models have come to be called regional climate models (RCMs). Some early studies were those of Giorgi and Bates (1989) over northern America, McGregor and Walsh (1993) over Australia, and Kida et al. (1991) over Japan. The resolution of RCMs is often around 50 km, but in recent years some studies have been performed at 10 km resolution or finer.

Another method for obtaining finer resolution climate change information is to use some form of statistical downscaling from dynamical climate models, typically from coupled atmosphere–ocean GCMs, though the technique may also be applied

to further downscaling RCM simulations. A feature of this type of methodology is that some error-correction (for present-day climate) may be incorporated. Both dynamical and statistical downscaling methods are discussed in the following subsections, and examples of their use over the Asian region are presented.

2.2.2 Regional Model Downscaling

2.2.2.1 Dynamical Downscaling

As mentioned, dynamical downscaling methodologies were first developed about 20 years ago. The original technique involved the use of limited-area models "nested" within outputs from a GCM. Over the last decade, an increasing number of researchers are also using variable-resolution global atmospheric models for dynamical downscaling purposes. The dynamical downscaling techniques may be broadly arranged into four groups, and all may be referred to as RCMs.

(a) *Limited-area models with lateral boundary forcing*
Climate simulations with this technique commenced about 20 years ago, and the technique continues to be widely used. The technique is a natural evolution from limited-area numerical weather prediction (NWP) models, which have been used for operational forecasting for some decades. Although NWP models are usually only run for forecasts of a few days, they are well-suited to longer simulations if there is a reasonable flow through the domain, and the domain is not so large as to allow undesired internal circulations to develop. Where there is some incompatibility between the internal flow, and the prescribed lateral boundary conditions, some unwanted reflections may occur, with associated spurious rainfall effects. It is common in such models to include a lateral boundary zone, with flow progressively damped near the boundaries, to suppress artificial reflections. Reviews of this type of model are provided by Giorgi and Mearns (1991) and McGregor (1997).

(b) *Limited-area model with internal forcing (or nudging)*
A development for limited-area models was proposed by Kida et al. (1991), to provide internal forcing (within the limited-area domain) of larger-length scale features, such that they remain consistent with flow features of similar scale in the host GCM. Lateral boundary forcing is usually also included in such models. This type of dynamical downscaling permits rather larger downscaled domains than (a), because the flow will be broadly consistent with that of the host model over the whole domain.

(c) *Stand-alone variable-resolution global models, run in time slice mode*
Application of variable-resolution global atmospheric models was first described by Déqué and Piedlievre (1995), using ARPEGE, an adaptation of the ECMWF IFS NWP model to regional climate modeling. A time-slice approach is often used, where initial conditions are taken from analyses or a host GCM, and

the simulation is "free-standing", forced only by sea surface temperatures (SSTs) and sea-ice from the host GCM. By correcting the monthly biases of the SSTs of the host GCM (as compared to present-day observed SSTs) and applying these same monthly SST bias corrections for the duration of the climate simulation, it is possible in principle to avoid replicating the circulation biases of the host GCM. This type of simulation is usually only modestly stretched, in order to avoid significant refraction effects of waves passing through regions of varying resolution (Caian and Geleyn 1997). An intercomparison by Fox-Rabinovitz et al. (2006) of four such models over northern America at 50 km resolution demonstrated the efficacy of the methodology.

Under this category can be included high-uniform-resolution atmospheric GCMs run in time-slice mode. A notable example is provided by the 20 km climate simulations of the MRI-AGCM3.2 (Mizuki et al. 2012). The Meteorological Research Institute of Japan (MRI) have also performed 60 km global time-slice simulations, as have CSIRO with conformal-cubic atmospheric model, or CCAM, (Nguyen et al. 2011a, b); the latter for an ensemble driven by IPCC AR4 bias-corrected SSTs.

(d) *Strongly-stretched variable-resolution global models*
It is possible to downscale the time-slice variable-resolution simulations of (c) to even finer resolution. The CSIRO group running CCAM have adopted this dynamical downscaling methodology. A long time-slice simulation is first performed as in (c). The larger-scale atmospheric variables of this simulation may then be applied periodically (for example, every 6 h) to drive a more strongly-stretched simulation. The forcing by the larger-scale variables may be conveniently performed by means of a digital filter (Thatcher and McGregor 2009). The technique may be repeated successively to obtain even finer-resolution dynamically-downscaled simulation.

Dynamical downscaling over Asia and the Pacific Islands is being carried out by many groups, using one or more of the above methods. Table 2.1 lists a number of the groups, arranged according to the four downscaling methodologies. The various models are listed, and the typical resolution being used.

2.2.2.2 Areas Needing Improvements in RCMs

The impacts and adaptation communities require estimates of the uncertainty of regional climate simulations. Even for a given GHG emissions scenario, the 23 models of the IPCC Fourth Assessment produced a wide range of regional climate outcomes. One may be able to reduce this range by considering the "most credible" of the coupled GCMs, for example by the quality of their present-day climate simulation, or their climatological performance for indices such as ENSO. This desirability to produce ensembles of simulations also applies to dynamical downscaling. It may variously be addressed by a multi-RCM approach (for example model intercomparisons such as RMIP and CORDEX), by using a single RCM to downscale a variety of host GCMs, or by using a variety of RCMs driven by a variety of host GCMs.

Table 2.1 Some examples of dynamical downscaling methods used in the Asia-Pacific region

Downscaling method	Institute	Typical resolution and duration	Modeled regions
Limited-area – boundary forced			
RIEMS, WRF	CAS	50 km	China
WRF	Nat. Univ. Sing.	50, 12.5 km, 150y	Singapore
RegCM3	CMA	20 km; 2×30y	China
	Kyungpook Nat. U.	50 km 2×75y	CORDEX-EA
PRECIS	IMHEN	25 km; 20y, 2×10y	Vietnam
	Univ. Keb. Malaysia	25 km 2×30y	Malaysia
HadGEM3-RA	KMA/Met Office	50 km	CORDEX-EA
Limited-area – internally forced			
MM5/SNURCM, WRF	Seoul Nat.Univ	50 km 2×75y	CORDEX-EA
RSM	Yonsei Univ.	50 km 2×75y	CORDEX-EA
NHRCM	MRI	5 km; 3×20y	Japan
Global variable res. – time slice			
CCAM	CSIRO	60 km 140y	Global
LMDZ	IIMT (Pune)	35 km	India
	CSIR-CMMACS	35 km	India
MRI-AGCM3.2	MRI	60 km, 20 km 2×25y	Global
HadGEM2A	KMA	60 km, 2×30y	Global
Global highly-variable res.			
CCAM	CSIRO	60, 50, 14, 8 km 140y	RMIP/CORDEX, Indonesia, Pacific Is.

Within individual RCMs, there is a need to improve the representation and parameterization of physical processes. The following lists some of the more important issues for the Asian region:

– Land-cover change (LCC) needs improved treatments and methodologies are needed for estimating the future evolution of LCC;
– Improvements of the land surface to consider urban effects, river routing, and other related processes;
– Improvements to deep and shallow convection, to improve the diurnal convective behavior, and improve the distribution of convective heating throughout the depth of the atmosphere;
– Possible use of convective super-parameterizations (Grabowski 2001) though as model resolution gets very fine (around 2 km), there should then be no need for any convective parameterization, as the processes are explicitly resolved;
– Improved aerosol schemes for both direct and indirect effects;
– Simulation of the carbon cycle, source and sinks of nutrients for both land and ocean;
– Refined resolution, to better represent small islands and the Maritime Continent; and
– Coupling to a mixed-layer ocean or, ideally, a regional ocean model.

2.2.2.3 Statistical Downscaling

There are broadly three common statistical downscaling methodologies:

(a) *Perfect Prognosis approach*
In this methodology, statistical relationships are sought from observations for variables in which there is high confidence, whilst ignoring those in which there is low confidence. The assumption is that the model simulation of the large-scale predictors is "perfect." Some of these models include a noise component to help capture variability and extremes.

(b) *Model Output Statistics approach*
Model Output Statistics (MOS) methods develop statistical relationships between simulated predictors and observed predictands. They are most often applied to climate-model simulated fields of the same variable being predicted. At their simplest, MOS methods provide a bias correction of the present-day simulated field to match the observations.

(c) *Weather Generator approach*
Weather generators are statistical models that produce random sequences of climate variables with statistical properties that match those of the observed variables.

The above categorization and the various approaches are described in some detail by Evans et al. (2012). When comparing outputs of dynamical and statistical downscaling for present-day climate, the statistical methods tend to be closer to observed station data and present-day climate (for example, Frost et al. 2011; Iizumi et al. 2011). This is to be expected from the nature of the statistical methods, which are derived by strongly taking into account the observed values. A major difficulty with statistical downscaling is that the future validity is not known of the present-day correlations upon which the techniques are based. A recommended downscaling approach is to use dynamical downscaling to reach as fine a resolution as can be achieved with available computing resources, then proceed to still-finer scales (for example, catchment or station scale) by means of statistical downscaling. Note that the final statistical downscaling step is able to remove the various biases of the dynamically-downscaled simulations (for example, Corney et al. 2010).

2.2.3 Asian Climate Change Projections

2.2.3.1 Projection of Asian Climate by GCMs

Generally, for the Asia-Pacific region, the IPCC Fourth Assessment Report (AR4) finds that future warming may lead to summer heat waves of longer duration and greater intensity frequency in East Asia with fewer very cold days in East Asia and

South Asia. It is also possible that precipitation will increase in northern areas and the Tibetan Plateau, as well as in eastern Asia and the southern parts of Southeast Asia (Christensen et al. 2007).

However, the climate across Asia is different from that in other areas because it is dominated by the most significant monsoon in the world. Traditionally, the Asian monsoon was separated into the south Asian monsoon, east Asian monsoon, western north Pacific monsoon and southeast Asian monsoon, depending on the different physical monsoon processes. Besides the heating contrast between land and ocean, ENSO is one of the key processes affecting the intensity of the southeast Asian monsoon and south Asian monsoon. At the same time, tropical cyclones bring moisture to Asian monsoon areas. The east Asian monsoon is thought to be influenced by the heat conditions over the Tibetan Plateau and the temperature gradient along the east coast, which means the western Pacific Ocean is important to the east Asian monsoon.

The east Asian summer monsoon shows typical characteristics of a rainy season in June and July, which is called Meiyu in China, Baiu in Japan and Changma in Korea. This Meiyu-Baiu-Changma front can be well represented in high resolution GCMs. Kitoh and Uchiyama (2006) found that the withdrawal of the Meiyu-Baiu-Changma rainy season may be delayed under climate change conditions; they used 15 GCM outputs under the IPCC A1B emissions scenario. By using a 20-km resolution atmospheric GCM, Kusunoki and Mizuta (2008) found increasing rainfall over the Yangtze River valley and western Japan may occur in the future. By checking CMIP3 modeling ensemble products under the A1B scenario, Ninomiya (2011) showed the northward shift of both Meiyu and Baiu fronts, and that the rainfall decreased slightly in twenty-first century projections.

It is noted in Sect. 2.1.4 that aerosols have a significant impact on climate across Asia owing to emissions from biomass burning and fossil fuel consumption. Wild's (2009b) study of Climate Model Intercomparison Project Phase 3 (CMIP3) models suggests that, while the models capture many features of the climate of the last 50 years, their decadal-scale variability is less than observed partly because they do not account for the variability of aerosols in the atmosphere.

CMIP3 remains an important source of model output to support a wide range of applications. However, recognizing that there is now an increased emphasis both on long-term projections to support mitigation scenarios and on short-term climate change a couple of decades ahead, the World Climate Research Programme (WCRP) has commenced a much broader set of model experiments as Phase 5 of CMIP (CMIP5). Taylor et al. (2012) provide a summary of the aims and plans for CMIP5, which will involve research institutes around the world including the Asia-Pacific region.

By analyzing outputs from eight CMIP5 models under the new scenarios (RCP 2.6, 4.5, 8.5 indicating low, middle, high emission scenarios), a study in China has found that the increase in global temperature over the present century (2006–2099) under the new scenarios is lower and the uncertainty range is less than for the corresponding AR4 scenarios. For example, the increase in global temperature is found to be around 1.4–2.2 °C over this century under RCP4.5 in CMIP5, while it is 1.7–4.4 °C in A1B scenario in CMIP4.

2.2.3.2 Projection of Asia-Pacific Climate by RCMs

Much information on climate projections for Asia can be found in the IPCC AR4 (2007a). In Chap. 11 (regional climate projection) of the Working Group 1 report, Asia is separated into six sub-areas, which are northern Asia (50–70°N, 40–180°E), Central Asia (30–50°N, 50–100°E), Tibetan Plateau (30–75°N, 50–100°E), East Asia (20–50°N, 100–145°E), South Asia (5–50°N, 64–100°E) and Southeast Asia (11°S–20°N, 95–115°E). Regarding the twenty-first century Asian climate projection for the A1B scenario in IPCC AR4, warming is found to be largest in high latitude (northern Asia, central Asia) and high altitude (Tibetan Plateau) regions; East Asia and South Asia are higher than the global mean, and southeast Asia is similar to the global mean. In most of the sub-areas of Asia, winter (December-February (DJF)) warming contributes more than other seasons; an exception is summer (June-August (JJA)) in Central Asia.

For precipitation changes due to enhanced GHG effects, a suppression of the south Asian summer monsoon, along with a delay of monsoon onset and increase of monsoon break periods are indicated by Ashfaq et al. (2009). In the research of Kumar et al. (2011) by analyzing the outputs from the PRECIS model, the model projections indicate significant warming over India towards the end of the twenty-first century. The summer monsoon precipitation over India is expected to be 9–16 % more in the 2080s compared to the baseline 1970s (1961–1990) under global warming conditions. Also, rainy days are projected to be less frequent and more intense over central India.

By using the ensemble results of five GCMs, Immerzeel et al. (2010) analyzed the impact of global warming on the water resources of the Himalayan river basins in the mid twenty-first century (2046–2065) under the A1B scenario. The Indus and Brahmaputra basins are found to be more influenced by climate warming than the Ganges, Yangtze and Yellow rivers, because the large population and large-scale irrigation heavily rely on melting water in these two areas. By using the CMIP3 and CMIP4 outputs, Wang and Zhang (2010) found that if there is extensive ice-melt in the Arctic under global warming then it is likely to result in stronger east Asian summer monsoons and more rainfall in northern China, north west China and the Maritime continent of Indonesia.

A recent study included running CCAM in time-slice mode at 60 km global resolution for the A2 emissions scenario, forced by the bias-corrected SSTs from an ensemble of six coupled GCMs from AR4 (Nguyen and McGregor 2009; Nguyen et al. 2011a, b). The pattern of warming of surface air temperature from the simulations is shown in Fig. 2.13 with largest oceanic increases over the equatorial region, showing similarities over the Pacific to the observed increases in recent decades as shown in Fig. 2.14. An analysis of the six CCAM ensemble members and their host GCMs suggests that the horizontal gradient of the surface sea-level pressure across the tropical Pacific will weaken under the warm future climate condition. This is consistent with a weakening of large-scale vertical circulations. The model simulations project indicates that the Pacific annual mean rainfall will significantly increase along the ITCZ, with weak changes elsewhere. For the southern

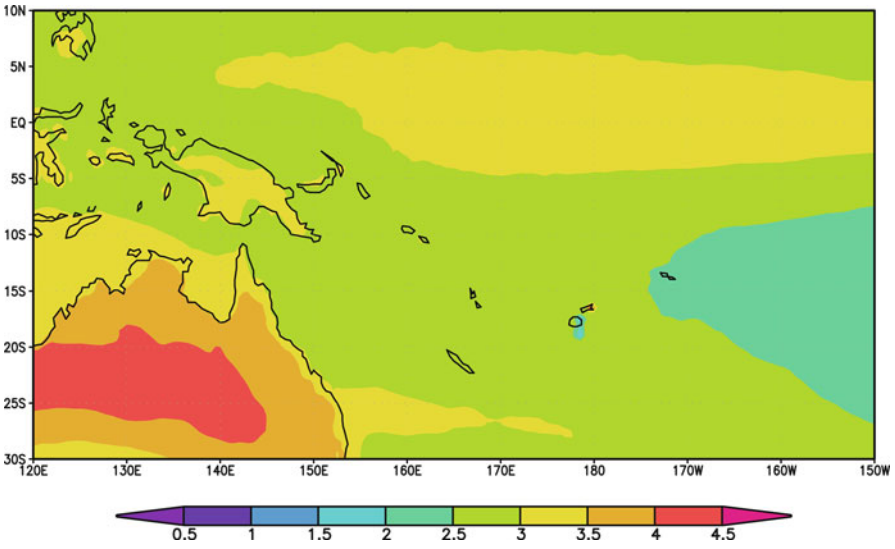

Fig. 2.13 Change in annual maximum near-surface air temperature (°C) 2080–2099 and 1980–1999 for the CCAM 60 km multi-model simulations using the A2 emission scenario (Created by J.M. McGregor with data from Nguyen et al. 2011a, b)

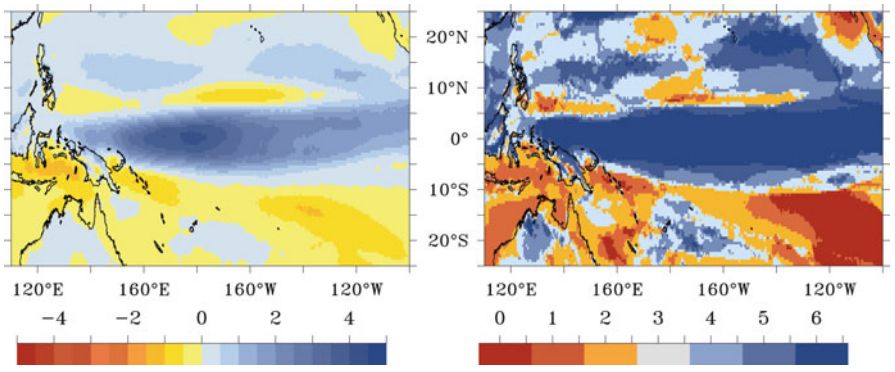

Fig. 2.14 Simulated annual change in rainfall (mm/day) between 2080 and 2099 and 1980–1999 (*left*) and amount of agreement of increase (*right*, *0* means all show decrease, *6* indicates all 6 model runs show increase). Results are for CCAM 60 km simulations for the A2 scenario, driven by SST changes of 6 AR4 coupled GCMs (Created by J.M. McGregor with data from Nguyen et al. 2011a, b)

hemisphere, rainfall is projected to decrease, with the largest reduction seen over the subtropical high. On the other hand, an increase in annual mean rainfall is projected for the northern hemisphere Pacific and over most land areas.

The situation appears somewhat different over the maritime continent region, with its complicated convective rainfall behavior, related to its many islands.

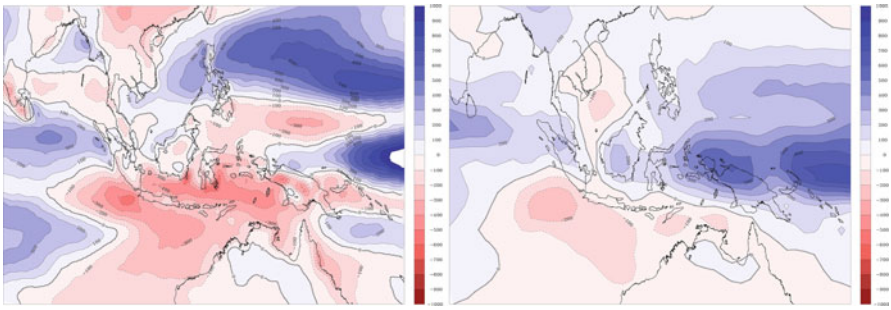

Fig. 2.15 Simulated average annual rainfall changes (changed mm/year amounts) in (2080–2100) compared to (1961–1990) from an ensemble of 60 km CCAM simulations over Indonesia (*left*, McGregor et al. 2009), and the six host GCMs (*right*) (Created by J.M. McGregor with data from Nguyen et al. 2011a, b)

In a downscaling study over the region using an ensemble of 60 km CCAM simulations driven by six of the AR4 coupled GCMs (McGregor et al. 2009), the ensemble of downscaled simulations, and also the host GCM ensemble, indicate a future reduction in annual rainfall (Fig. 2.15) for most of the larger islands of the maritime continent.

2.2.4 Coordinated Projects on Regional Modeling

Many research groups now run either global or regional climate models for climate research or for the support of climate impact studies. Through regional collaboration such groups have developed inter-comparison programs that compare the results of an individual model with those of all other models as well as with region climate observations (Wang 2012). These coordinated projects allow the uncertainties in model results to be quantified and hence develop confidence in the application of models to climate impact studies.

2.2.4.1 Regional Model Intercomparison Project (RMIP)

The Regional Climate Model Intercomparison Project (RMIP) involves long-term regional coordination on Asian climate change studies (Fu et al. 2005). It has three phases, each focusing on different scientific objectives. Phases I and II were designed to assess the ability of models to simulate the seasonal cycle, climate extremes, and general climatology across Asia (Fu et al. 2005; Lee et al. 2007; Feng et al. 2011b; Feng and Fu 2006).

In 2009, RMIP III on "Building Asian Climate Change Scenarios by Multi-Regional Climate Models Ensemble" was established and, at the time of writing, is continuing with financial support from the APN (Wang and Zhang 2010). The objective of

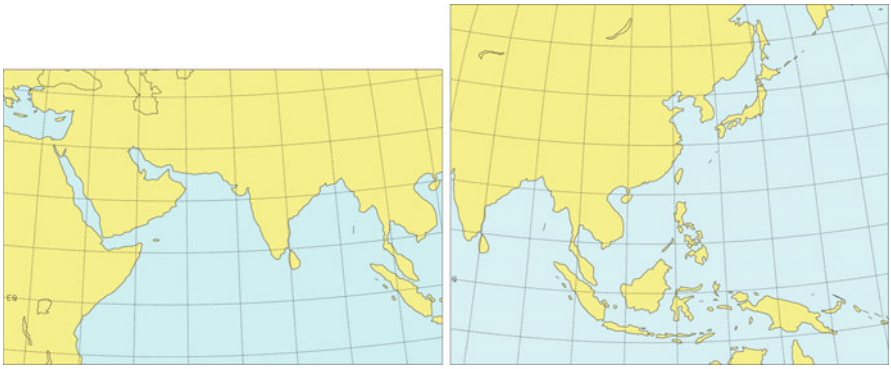

Fig. 2.16 CORDEX domains for West Asia and East Asia; each have about 50 km grid resolution (Plotted using the domain specifications available at http://wcrp-cordex.ipsl.jussieu.fr)

RMIP III is to generate robust climate change scenarios for the impact and adaptation research communities, including detailed evaluation and assessment of the source and magnitude of uncertainties. The project also aims to increase the understanding of variability of the east Asia monsoon system in future climate and its impact on regional climate.

Ten RCMs and two GCMs from seven regional climate modeling groups across the Asia-Pacific region are participating in RMIP III. The CORDEX East Asia domain is adopted for the study, and two time slices are composed of present-day conditions (1900–2000) and future climate (2000–2070).

2.2.4.2 Coordinated Regional Downscaling Experiment (CORDEX)

A WCRP initiative in partnership with START and other key institutions, CORDEX aims to produce climate information at regional to local scales to help and support local decision makers respond to potential climate change. Even though there exist several successful intercomparison programs for each continent (for example, ENSEMBLE over Europe, PIRCS and NARCAPP over North America, RMIP over Asia), the strength of CORDEX compared to previous projects is to provide a common framework in a global-wide perspective for regional climate projections in order to understand their uncertainties as well as provide model evaluation (Giorgi et al. 2009). The domain size for East Asia (Fig. 2.16) is the largest among the 12 domains of CORDEX. This large domain may lead to problems both scientifically and practically. Nevertheless, the benefit of this domain is that the CORDEX-East Asia domain covers the maritime continent in the western Pacific, which is a somewhat vulnerable area with respect to climate change. South Asia has its own large CORDEX domain, with coordination of the simulations and analyses being undertaken at the Indian Institute of Tropical Meteorology (IITM). IITM has a particular interest in long-term monsoon change and modeling of the south Asian monsoon.

The Korea Meteorological Administration (KMA) is participating in CORDEX, in collaboration with the UK Met Office Hadley Centre. Four dynamical regional climate models and one statistical model are involved in this collaborative research. Phase I (2010–2011) focuses on the CORDEX-East Asia domain with 50 km resolution and Phase II (2012~) focuses on the area of the Korean peninsula but with resolution 12.5 km or finer. The strategy of CORDEX includes current climate simulations and regional projections forced by CMIP5 global projections based on Representative Concentration Pathways (RCP) emission scenarios.

2.2.5 Applications and Case Studies

This sub-section introduces some successful cases of regional climate projection.

2.2.5.1 RMIP

Based on the evaluation of the ability of RCMs to simulate Asian climate on different time scales in RMIP I and II (Fu et al. 2005; Feng and Fu 2006; Lee, et al. 2007; Feng et al. 2011c), RMIP III considers projections of Asian climate change for the period 2040–2070. Compared with the present-day climate (1980–2000), initial results from nine RCMs suggest that annual Asian surface air temperature will increase by 2.0 °C around 2050, with more warming in the winter season (DJF) of 2.1 °C. Precipitation is expected to increase by about 2.4 % annually, with a greater increase over land.

2.2.5.2 Adapting Climate Change in China (ACCC) project

The Adapting Climate Change in China (ACCC) project is an international project focused on understanding the impact of climate change on Chinese agriculture, such as the risk of droughts, extreme weather events, increasing temperatures and changes in water availability. The ACCC project expects to promote and enhance climate change adaptation capacity of local policy makers and the general public. These aims are achieved through improving climate science and impact assessments, and incorporating the views of local communities and decision-makers on potential adaptation responses to climate impacts. The UK Meteorological Office's use of their PRECIS modeling system has produced high-resolution downscaled future scenarios in a dryland area of China (Ningxia Province, China) to be used in an assessment study of agricultural production and water management. Vulnerability indicators for dryland, water and agriculture sectors were developed and the vulnerability assessment methodology was used by scientists and local policy makers in the Adapting to Climate Change in China Project (see http://www.ccadaptation.org.cn/en/index.aspx).

2.2.5.3 Pacific Climate Change Science Program

The Pacific Climate Change Science Program (PCCSP) was initiated and funded by the Government of Australia. Under this program, the Australian Bureau of Meteorology and Commonwealth Scientific and Industrial Research Organisation (2011) conducted a comprehensive modeling and impacts study for 15 of the Pacific's island countries. Projects under the PCCSP included both dynamical and statistical downscaling, and produced impacts and adaptation advice for these countries to facilitate effective adaptation planning and implementation (Power et al. 2011).

2.3 Conclusions

The geographic extent of Asia and the Pacific leads to great variation in the climate of the region. Major influences on global climate arise from the scale and elevation of the Himalayas Tibetan Plateau (HTP), and from the air-sea interactions in the Pacific associated with the El Niño–Southern Oscillation (ENSO). The monsoon has a profound effect on the climate of Asia, with its strong seasonal cycle driving a range of human activities, especially agriculture, as well as the life-cycles of natural ecosystems.

Climate observations show significant trends in temperature across Asia and the Pacific; not only is there an increase in mean temperature but also in extremes such as the frequency of hot days. Observed trends in precipitation are more variable, but there is some evidence of increasing intensity of storms. Projections of future climate change for the region suggest longer summer heat waves in East Asia and increases in precipitation in several areas.

Our understanding of the climate of the region is critically dependent on the availability and quality of observations of the atmosphere, ocean and land surface, and so it is essential for such data to be collected and analyzed routinely and carefully. Because of the complex interactions of the climate system, these data cannot be usefully studies in isolation and so there needs to be sharing of climate data and associated expertise across the whole region.

Even collecting climate data in some parts of the region is challenging. For example, the isolation of some islands of the Pacific makes routine observation difficult, while the terrain and climate of the Himalayas give rise to an unfriendly environment for routine measurement. Cooperation at regional and international levels needs to be promoted to ensure that an effective record of the climate of the region is maintained.

Numerical modeling provides a means for assimilating observations in a dynamically consistent manner and for then making predictions of future weather and climate. A number of major centers in Asia and the Pacific maintain complex climate modeling systems, and these groups generally collaborate with similar agencies around the world through projects such as the Coupled Model Intercomparison Project (CMIP). Such projects are important in ensuring the quality of model output, and in promoting the development of model improvements.

However, modeling as a tool for the support of climate impact and adaptation studies is of interest to many groups across the region. Regional climate models can be used for this purpose, and these models can be used by a wide range of groups to 'downscale' the output of global models to local scales. Downscaling can also be achieved through statistical methods, which are readily accessible to the broad science community. Projects like the Coordinated Regional Downscaling Experiment (CORDEX) provide a means to promote cooperation across the modeling and climate applications communities.

References

Ashfaq, M., Shi, Y., Tung, W. W., Trapp, R. J., Gao, X., Pal, J. S., & Diffenbaugh, N. S. (2009). Suppression of south Asian summer monsoon precipitation in the 21st century. *Geophysical Research Letters, 36*, L01704. doi:10.1029/2008GL036500.

Australian Bureau of Meteorology & CSIRO. (2011). *Climate change in the Pacific: Scientific assessment and new research.* Volume 1: Regional overview. Volume 2: Country reports.

Baidya, S. K., Shrestha, M. L., & Sheikh, M. M. (2008). Trend in daily climatic extremes of temperature and precipitation in Nepal. *Journal of Hydrology and Meteorology, 5*(1), 38–51. SOHAM-Nepal.

Bohannon, J. (2008). The big thaw reaches Mongolia's pristine north. *Science, 319*, 567–568.

Burgman, R. J., Clement, A. C., Mitas, C. M., Chen, J., & Esslinger, K. (2008). Evidence for atmospheric variability over the Pacific on decadal timescales. *Geophysical Research Letters, 35*, L01704. doi:10.1029/2007GL031830.

Caian, M., & Geleyn, J. -F. (1997). Some limits to the variable-mesh solution and comparison with the nested-LAM solution. *Quarterly Journal of the Royal Meteorological Society, 123*, 743–766.

Chinn, T., Fitzharris, B. B., Willsman, A., & Salinger, J. (2012). Annual ice volume changes 1976–2008 for the New Zealand Southern Alps. *Global and Planetary Change, 92*. doi:10.1016/j.gloplacha.2012.03.002.

Christensen, J. L., Hewitson, B., Busuioc, A., Chen, A., Gao, X., Held, I., … & Kumar K. (2007). Regional climate projections. Climate change 2007: The scientific basis. Contribution of working group I to the fourth assessment report of the intergovernmental panel on climate change. In S. Solomon, D. Qin, M. Manning, Z. Chen, K. Averyt, M. Marquis, K. B. M. Tignor & H. L. Miller (Eds.) (pp. 847–940). Cambridge: Cambridge University Press.

Clark, C. O., Webster, P. J., & Cole, J. E. (2003). Interdecadal variability of the relationship between the Indian Ocean zonal mode and East African coastal rainfall anomalies. *Journal of Climate, 16*, 548–554.

Cogley, J. G., Kargel, J. S., Kaser, G., & Van der Veen, C. J. (2010). Tracking the source of glacier misinformation. *Science, 327*, 522.

Corney, S. P., Katzfey, J. J., McGregor, J. L., Grose, M. R., Bennett, J., White, C. J., … & Bindoff, N. L. (2010). *Climate futures for Tasmania: Modelling technical report*. Hobart: Antarctic Climate and Ecosystems Cooperative Research Centre.

Cruz, R. V., Harasawa, H., Lal, M., Wu, S., Anokhin, Y., Punsalmaa, B., … & Huu Ninh, N. (2007). Asia. Climate change 2007: Impacts, adaptation and vulnerability. Contribution of working group II to the Fourth Assessment Report of the Intergovernmental Panel on Climate Change. In M.L. Parry, O.F. Canziani, J.P. Palutikof, P.J. van der Linden, & C.E. Hanson (Eds.) (pp. 469–506). Cambridge: Cambridge University Press.

Déqué, M., & Piedlievre, J. P. (1995). High resolution climate simulation over Europe. *Climate Dynamics, 11*, 321–339.

Deser, C., Phillips, A. S., & Hurrell, J. W. (2004). Pacific interdecadal climate variability: Linkages between the tropics and the north Pacific during boreal winter since 1900. *Journal of Climate, 17*, 3109–3124.

Evans, J., McGregor, J. L., & McGuffie, K. (2012). Future regional climates. In H. Henderson-Sellers, & K. McGuffie (Eds.), *Future of the World's climate*. Elsevier, 223–252.

Feng, J., & Fu, C. (2006). Inter-comparison of 10-year precipitation simulated by several RCMs for Asia. *Advances in Atmospheric Sciences, 23*(4), 531–542.

Feng, R., et al. (2011a). Regime change of the boreal summer Hadley circulation and its connection with the tropical SST. *Journal of Climate, 24*, 3867–3877. doi:10.1175/2011JCLI3959.1.

Feng, J. M., Wang, Y. L., & Fu, C. (2011b). Simulation of extreme climate events over China with different regional climate models. *Atmospheric and Oceanic Science Letters, 4*(1), 47–56.

Feng, J., Lee, D. K., Fu, C., Tang, J., Sato, Y., Kato, H., … & Mabuchi, K. (2011c). Comparison of four ensemble methods combining regional climate simulations over Asia. *Meteorology and Atmospheric Physics, 11*(1–2), 41–53. doi:10.1007/s00703-010-0115-7.

Folland, C. K., Renwick, J. A., Salinger, M. J., & Mullan, A. B. (2002). Relative influences of Zone. *Geophysical Research Letters, 29*, 1643. doi:10.1029/2001GL014201.

Fox-Rabinovitz, M., Côté, J., Dugas, B., Déqué, M., & McGregor, J. L. (2006). Variable resolution general circulation models: Stretched-grid model intercomparison project (SGMIP). *Journal of Geophysical Research, 111*, D16104. doi:10.1029/2005JD006520.

Frost, A. J., Charles, S. P., Timbal, B., Chiew, F. H. S., Mehrotra, R., Nguyen, K. C., … & Kent, D. M. (2011). A comparison of multi-site daily rainfall downscaling techniques under Australian conditions. *Journal of Hydrology*, *408*(1–2), 1–18. doi:10.1016/j.jhydrol.2011.06.021.

Fu, C., Wang, S., Xiong, Z., Gutowski, W. J., Lee, D. K., McGregor, J. L., … & Suh, M.S. (2005). Regional climate model intercomparison project for Asia. *Bulletin of the American Meteorological Society*, *86*, 257–266.

Fujii, Y., Nakawo, M., & Shrestha, M. L. (1976). Mass balance studies of the glaciers in hidden valley, Mukut Himal. *Journal of the Japanese Society of Snow and Ice, 38*, 17–21.

Fujii, Y., Fujita, K., & Paudyal, P. (1996). Glaciological research in hidden valley, Mukut Himal in 1994. *Bulletin of Glacier Research, 14*, 7–11.

Fujita, K., & Nuimura, T. (2011). Spatially heterogeneous wastage of Himalayan glaciers. *PNAS, 108*(34), 14011–14014.

Gadgil, S. (2003). The Indian monsoon and its variability. *Annual Review of Earth and Planetary Sciences, 31*, 429–467.

Giorgi, F., & Bates, G. T. (1989). On the climatological skill of a regional model over complex terrain. *Monthly Weather Review, 117*, 2325–2347.

Giorgi, F., & Mearns, L. O. (1991). Approaches to the simulation of regional climate change: A review. *Reviews of Geophysics, 29*, 191–216.

Giorgi, F., Jones, C., & Asrar, G. R. (2009). Addressing climate information needs at the regional level: The CORDEX framework. *WMO Bulletin, 58*(3), 175–183.

Goswami, B. N., Wu, G., & Yasunari, T. (2006a). The annual cycle, intraseasonal oscillations, and roadblock to seasonal predictability of the Asian summer monsoon. *Journal of Climate, 19*, 5078–5099. doi:10.1175/JCLI3901.1.

Goswami, B. N., Venugopal, V., Sengupta, D., Madhusoodanan, M. S., & Xavier, P. K. (2006b). Increasing trend of extreme rain events over India in a warming environment. *Science, 314*(5804), 1442–1445. doi:10.1126/science.1132027.

Goswami, B. N., Kulkarni, J. R., Mujumdar, V. R., & Chattopadhyay, R. (2010). On factors responsible for recent secular trend in the onset phase of monsoon intraseasonal oscillations. *International Journal of Climatology, 30*, 2240–2246. doi:10.1002/joc.2041.

Grabowski, W. W. (2001). Coupling cloud processes with the large-scale dynamics using the Cloud-Resolving Convection Parameterization (CRCP). *Journal of the Atmospheric Sciences, 58*, 978–997.

Higuchi, K., Iozawa, T., & Higuchi, H. (1976). Flight observations for the inventory of glaciers in the Nepal Himalaya. *Journal of the Japanese Society of Snow and Ice, 38*, 6–9.

Iizumi, T., Nishimori, M., Dairaku, K., Adachi, S. A., & Yokozawa, M. (2011). Evaluation and intercomparison of downscaled daily precipitation indices over Japan in present-day climate: Strengths and weaknesses of dynamical and bias correction-type statistical downscaling methods. *Journal of Geophysical Research, 116*, D01111. doi:10.1029/2010JD014513.

Immerzeel, W. W., van Beek, L. P. H., & Bierkens, M. F. P. (2010). Climate change will affect the Asian water towers. *Science, 328*, 1382–1385.

IPCC. (2007a). In S. Solomon, D. Qin, M. Manning, Z. Chen, M. Marquis, K. B. Averyt, M. Tignor, & H. L. Miller (Eds.), *Climate change 2007: The physical science basis, Contribution of working group I to the Fourth Assessment Report of the Intergovernmental Panel on Climate Change*. Cambridge, UK/New York: Cambridge University Press.

IPCC. (2007b). Summary for policymakers. In S. Solomon, D. Qin, M. Manning, Z. Chen, M. Marquis, K. B. Averyt, M. Tignor, & H. L. Miller (Eds.), *Climate change 2007: The physical science basis. Contribution of working group I to the Fourth Assessment Report of the Intergovernmental Panel on Climate Change*. Cambridge, UK/New York: Cambridge University Press.

IPCC. (2012). In C. B. Field, V. Barros, T. F. Stocker, D. Qin, D. J. Dokken, K. L. Ebi, M. D. Mastrandrea, K. J. Mach, G.-K. Plattner, S. K. Allen, M. Tignor, & P. M. Midgley (Eds.), *Managing the risks of extreme events and disasters to advance climate change adaptation. A Special report of working groups I and II of the Intergovernmental Panel on Climate Change*. Cambridge, UK/New York: Cambridge University Press.

Ives, J. D., Shrestha, R. B., & Mool, P. K. (2010). *Formation of glacial lakes in the Hindu Kush-Himalayas and GLOF risk assessment*. Kathmandu: ICIMOD.

Johanson, C. M., & Fu, Q. (2009). Hadley cell widening: Model simulations versus observations. *Journal of Climate, 2*, 2713–2725.

Johansson, A. (2007). Prediction skill of the NAO and PNA from daily to seasonal time scales. *Journal of Climate, 20*, 1957–1975.

Joshi, U. R., & Rajeevan, M. (2006). *Trends in precipitation extremes over India* (Research report, Vol. 3/2006). Pune: Indian Meteorological Department.

Kent, D. M., Kirono, D. G. C., Timbal, B., & Chiew, F. H. S. (2011). Representation of the Australian sub-tropical ridge in the CMIP3 models. *International Journal of Climatology, 33*(1), 48–57. doi:10.1002/joc.3406.

Kida, H., Koide, T., Sasaki, H., & Chiba, M. (1991). A new approach for coupling a limited area model to a GCM for regional climate simulations. *Journal of the Meteorological Society of Japan, 69*, 723–728.

Kidson, J. W. (1999). Principal modes of Southern Hemisphere low frequency variability obtained from NCEP-NCAR reanalyses. *Journal of Climate, 12*, 2808–2830.

Kiladis, G. N., von Storch, H., & van Loon, H. (1989). Origin of the South Pacific convergence zone. *Journal of Climate, 2*, 1185–1195.

Kinter, J. L., Miyakoda, K., & Yang, S. (2002). Recent change in the connection from the Asian monsoon to ENSO. *Journal of Climate, 15*, 1203–1215.

Kitoh, A., & Uchiyama, T. (2006). Changes in onset and withdrawal of the East Asian summer rainy season by multi-model global warming experiments. *Journal of the Meteorological Society of Japan, 84*, 247–258.

Knutson, T. R., McBride, J. L., Chan, J., Emanuel, K., Holland, G., Landsea, C., … & Sugi, M. (2010). Tropical cyclones and climate change. *Nature Geoscience, 3*, 157–163.

Können, G. P., Jones, P. D., Kaltofen, M. H., & Allan, R. J. (1998). Pre-1866 extensions of the Southern Oscillation index using early Indonesian and Tahitian meteorological readings. *Journal of Climate, 11*, 2325–2339.

Kothawale, J. V., Revasdekar, J. V., & Kumar, K. R. (2009). Recent trends in pre-monsoon daily temperature extremes over India. *Journal of Earth System Science, 119*(1), 51–65.

Krishnamurthy, V., & Goswami, B. N. (2000). Indian monsoon-ENSO relationship on interdecadal timescale. *Journal of Climate, 13*, 579–595.

Kumar, R., Areendran, G., & Rao, P. (2009). Witnessing change: Glaciers in the Indian Himalayas. Pilani, WWF-India and Birla Institute of Technology.

Kumar, K. K., Patwardhan, S. K., Kulkarni, A., Kamala, K., Rao, K. K., & Jones, R. (2011). Simulated projections for summer monsoon climate over India by a high-resolution regional climate model (PRECIS). *Current Science, 101*, 312–326.

Kusunoki, S., & Mizuta, R. (2008). Future changes in the Baiu rain band projected by a 20-km mesh global atmosphere model: Sea surface temperature dependence. *SOLA, 4*, 85–88.

Kwon, W. T. (2007) Development of indices and indicators for monitoring trends in climate extremes and its application to climate change projection. (APN Project Report for APN project: ARCP2007-20NSG). Retrieved from http://www.apn-gcr.org/resources/items/show/1537

Lambert, S.J., & Fyfe, J.C. (2006). Changes in winter cyclone frequencies and strengths simulated in enhanced greenhouse warming experiments: results from the models participating in the IPCC diagnostic exercise. *Climate Dynamics, 26*, 713–728.

Larkin, N. K., & Harrison, D. E. (2005). On the definition of El Niño and associated seasonal average U.S. weather anomalies. *Geophysical Research Letters, 32*, L13705. doi:10.1029/2005GL022738.

Lau, K. M., & Nath, M. J. (2000). Impact of ENSO on the variability of the Asian–Australian monsoons as simulated in GCM experiments. *Journal of Climate, 13*, 4287–4309.

Lau, N. C., & Nath, M. (2004). Coupled GCM simulation of atmosphere–ocean variability associated with zonally asymmetric SST changes in the tropical Indian Ocean. *Journal of Climate, 17*, 245–265.

Lee, D.-K., Gutowski, W., Kang, H. S., & Kim, C. J. (2007). Intercomparison of precipitation simulated by regional climate models over East Asia in 1997 and 1998. *Advances in Atmospheric Sciences, 24*(4), 539–554.

Li, J. P., Zhu, Z. W., Jiang, Z. H., & He, J. H. (2010). Can global warming strengthen the East Asian summer monsoon? *Journal of Climate, 23*, 6696–6705. doi:10.1175/2010JCLI3434.1.

Liu, S. C., Fu, C., Shiu, C.-J., Chen, J.-P., & Wu, F. (2009). Temperature dependence of global precipitation extremes. *Geophysical Research Letters, 36*, L17702.

Lucas, C., Nguyen, H., & Timbal, B. (2012). An observational analysis of Southern Hemisphere tropical expansion. *Journal of Geophysical Research, 117*, D17112. doi:10.1029/2011JD017033.

Manton, M. J., Della–Marta, P. M., Haylock, M. R., Hennessy, K. J., Nicholls, N., Chambers, L. E., … & Yee, D. (2001). Trends in extreme daily rainfall and temperature in Southeast Asia and the south Pacific: 1961–1998. *International Journal of Climatology, 21*, 269–284.

Mantua, N. J., Hare, S. R., Zhang, Y., Wallace, J. M., & Francis, R. C. (1997). A Pacific interdecadal climate oscillation with impacts on salmon production. *Bulletin of the American Meteorological Society, 78*, 1069–1079.

McGregor, J. L. (1997). Regional climate modelling. *Meteorology and Atmospheric Physics, 63*, 105–117.

McGregor, J. L., & Walsh, K. (1993). Nested simulations of perpetual January climate over the Australian region. *Journal of Geophysical Research, 98*, 23283–23290.

McGregor, J. L., Nguyen, K., Katzfey, J. J., & Thatcher, M. (2009). Regional climate modelling over island countries. Extended abstracts, international symposium on equatorial monsoon system, Kuta Paradiso Hotel, Bali, 16–18 July 2009.

McPhaden, M. J. (2004). Evolution of the 2002/03 El Niño. *Bulletin of the American Meteorological Society, 85*, 677–695.

McPhaden, M. J., Zebiak, S. E., & Glantz, M. H. (2006). ENSO as an integrating concept in earth science. *Science, 314*, 1740–1745.

Mizuta, R., Yoshimura, H., Murakami, H., Matsueda, M., Endo, H., Ose, T., Kamiguchi, K., Hosaka, M., Sugi, M., Yukimoto, S. Kusunoki, S. & Kitoh, A. (2012). Climate simulations using MRI-AGCM3.2 with 20-km grid. *Journal of the Meteorological Society of Japan, 90A*, 233–258.

Muller, F. (1970). Inventory of glaciers in the Mount Everest region. In *Perennial ice and snow masses* (Technical papers in hydrology, Vol. 1, pp. 47–59). Paris: UNESCO/IAHS.

Nakajima, T., Yoon, S. C., Ramanathan, V., Shi, G. Y., Takemura, T., Higurashi, A., … & Schutgens, N. (2007). Overview of the Atmospheric Brown Cloud East Asian Regional Experiment 2005 and a study of the aerosol direct radiative forcing in East Asia. *Journal of Geophysical Research*, *112*(D24), D24S91.

Nakawo, M., Fujii, Y., & Shrestha, M. L. (1976). Flow of glaciers in hidden valley, Mukut Himal. *Seppyo, 38*, 39–43.

Nguyen, K. C., & McGregor, J. L. (2009). Modelling the Asian summer monsoon using CCAM. *Climate Dynamics, 32*, 219–236.

Nguyen, K., Katzfey, J. J., & McGregor, J. (2011a). Climate change projections based on downscaling. In G. Cambers. (Ed). *Climate change in the Pacific*. Pacific Climate Change Science Program Technical Report.

Nguyen, K. C., Katzfey, J. J., & McGregor, J. L. (2011b). Global 60 km simulations with CCAM: Evaluation over the tropics. *Climate Dynamics*. doi:10.1007/s00382-011-1197-8.

Ninomiya, K. (2011). Characteristics of the Meiyu and Baiu frontal precipitation zone in the CMIP3 20th century simulation and 21st century projection. *Journal of the Meteorological Society of Japan, 89*, 151–159.

Parthasarathy, B., Munot, A. A., & Kothawale, D. R. (1994). All India monthly and seasonal rainfall series: 1871–1993. *Theoretical and Applied Climatology, 49*, 217–224.

Power, S., Casey, T., Folland, C., Colman, A., & Mehta, V. (1999). Interdecadal modulation of the impact of ENSO on Australia. *Climate Dynamics, 15*, 319–324.

Power, S. B., Schiller, A., Cambers, G., Jones, D., & Hennessy, K. (2011). The Pacific climate change science program. *Bulletin of the American Meteorological Society, 92*, 1409–1411.

Qin, D., Liu, S., & Li, P. (2006). Snow cover distribution, variability, and response to climate change in Western China. *Journal of Climate, 19*, 1820–1833.

Ramanathan, V., Chung, C., Kim, D., Bettge, T., Buja, L., Kiehl, J. T., Washington, W. M., … & Wild, M. (2005). Atmospheric brown clouds: Impacts on South Asian climate and hydrological cycle. *Proceedings of the National Academy of Sciences of the United States of America, 102*, 5326–5333.

Ramanathan, V., Ramana, M. V., Roberts, G., Kim, D., Corrigan, C., Chung, C., & Winker, D. (2007). Warming trends in Asia amplified by brown cloud solar absorption. *Nature, 448*, 575–578.

Saji, N. H., Goswami, B. N., Vinayachandran, P. N., & Yamagata, T. (1999). A dipole mode in the tropical Indian Ocean. *Nature, 401*, 360–363.

Salinger, M. J., Basher, R. E., Fitzharris, B. B., Hay, J. E., Jones, P. D., MacVeigh, J. P., & Leleu, I. (1995). Climate trends in the south-west Pacific. *International Journal of Climatology, 15*, 285–302.

Shrestha, M. L., Fujii, Y., & Nakawo, M. (1976). Climate of hidden valley, Mukut Himal during the monsoon in 1974. *Journal of the Japanese Society of Snow and Ice, 38*, 105–108.

Smith, T. M., & Reynolds, R. W. (2005). A global merged land and sea surface temperature reconstruction based on historical observations (1880–1997). *Journal of Climate, 18*, 2021–2036.

Stevenson, S., Fox-Kemper, B., Jochum, M., Neale, R., Deser, C., & Meehl, G. (2011). Will there be a significant change to El Niño in the 21st century? *Journal of Climate, 25*, 2129–2145. doi:10.1175/JCLI-D-11-00252.1.

Straus, D. M., & Shukla, J. (2002). Does ENSO force the PNA? *Journal of Climate, 15*, 2340–2358.

Streten, N. A., & Troup, A. J. (1973). A synoptic climatology of satellite observed cloud vortices over the Southern Hemisphere. *Quarterly Journal of the Royal Meteorological Society, 99*, 56–72.

Streten, N. A., & Zillman, J. W. (1984). Climate of the South Pacific Ocean. In H. van Loon (Ed.), *Climates of the oceans, World survey of climatology volume 15* (pp. 263–429). Amsterdam: Elsevier.

Tanaka, H. L., Ishizaki, N., & Nohara, N. (2005). Intercomparison of the intensities and trends of Hadley, Walker and Monsoon Circulations in the global warming predictions. *Scientific Online Letters on the Atmosphere, 1*, 77–80.

Taylor, K. E., Stouffer, R. J., & Meehl, G. A. (2012). An overview of CMIP5 and the experimental design. *Bulletin of the American Meteorological Society, 9*, 485–498. doi:10.1175/BAMS-D-11-00094.1.

Terada, K., & Hanzawa, M. (1984). Climate of the North Pacific Ocean. In H. van Loon (Ed.), *Climates of the oceans, World survey of climatology volume 15* (pp. 431–503). Amsterdam: Elsevier.

Terray, P., Dominiak, S., & Delecluse, P. (2005). Role of the southern Indian Ocean in the transition of the monsoon-ENSO system during recent decades. *Climate Dynamics, 24*, 169–195.

Thatcher, M., & McGregor, J. L. (2009). Using a scale-selective filter for dynamical downscaling with the conformal cubic atmospheric model. *Monthly Weather Review, 137*, 1742–1752.

Timbal, B. & Drosdowsky, W. (2012). The relationship between the decline of Southeastern Australian rainfall and the strengthening of the subtropical ridge. doi:10.1002/joc.3492

Trenberth, K. E. (1976). Spatial and temporal variations of the Southern Oscillation. *Quarterly Journal of the Royal Meteorological Society, 102*, 639–653.

Trenberth, K. E. (1984). Signal versus noise in the Southern Oscillation. *Monthly Weather Review, 112*, 326–332.

Trenberth, K. E. (1990). Recent observed interdecadal climate changes in the Northern Hemisphere. *Bulletin of the American Meteorological Society, 71*, 988–993.

Trenberth, K. E. (1991). General characteristics of El Niño-Southern Oscillation. In M. H. Glantz, R. W. Katz, & N. Nicholls (Eds.), *Teleconnections linking worldwide climate anomalies. Scientific basis and societal impact* (pp. 13–42). Cambridge, UK: Cambridge University Press.

Trenberth, K. E. (1997). The definition of El Niño. *Bulletin of the American Meteorological Society, 78*, 2771–2777.

Trenberth, K. E., & Caron, J. M. (2000). The Southern Oscillation revisited: Sea level pressures, surface temperatures and precipitation. *Journal of Climate, 13*, 4358–4365.

Trenberth, K. E., & Stepaniak, D. P. (2001). Indices of El Niño evolution. *Journal of Climate, 14*, 1697–1701.

Trenberth, K. E., Caron, J. M., Stepaniak, D. P., & Worley, S. (2002). The evolution of ENSO and global atmospheric surface temperatures. *Journal of Geophysical Research, 107*, D8. doi:10.1029/2000JD000298. http://www.cgd.ucar.edu/cas/papers/2000JD000298.pdf.

Trenberth, K. E., Jones, P. D., Ambenje, P., Bojariu, R., Easterling, D., Tank, A. K., … & Zhai, P. (2007). Observations: Surface and atmospheric climate change. In S. Solomon, D. Qin, M. Manning, Z. Chen, M. Marquis, K. B. Averyt, M. Tignor, & H. L. Miller. (Eds.), *Climate change 2007: The physical science basis. Contribution of working group I to the Fourth Assessment Report of the Intergovernmental Panel on Climate Change* (pp. 235–336). Cambridge, UK/New York: Cambridge University Press.

Troup, A. J. (1965). The Southern Oscillation. *Quarterly Journal of the Royal Meteorological Society, 91*, 490–506.

Vincent, D. G. (1994). The South Pacific Convergence Zone (SPCZ): A review. *Monthly Weather Review, 122*, 1949–1970.

Wallace, J. M., & Gutzler, D. S. (1981). Teleconnections in the geopotential height field during the northern hemisphere winter. *Monthly Weather Review, 109*, 784–812.

Wang, S. (2012.) Building Asian climate change scenarios by regional climate models ensemble. (APN Project Report: ARCP2011-01CMY-Wang). Retrieved from http://www.apn-gcr.org/resources/items/show/1567

Wang, B., & Lin, H. (2002). Rainy season of the Asian–Pacific summer monsoon. *Journal of Climate, 15*, 386–398.

Wang, H., & Zhang, Y. (2010). Model projections of east Asian summer monsoon climate under "free Arctic" scenario. *Atmospheric and Oceanic Science Letters, 3*, 176–180.

Watanabe, O. (1976). On the types of glaciers in the Nepal Himalayas and their characteristics. *Journal of the Japanese Society of Snow and Ice, 38*, 10–16.

Watanabe, O., Endo, Y., & Ishida, T. (1967). Glaciers and glaciations in the Nepal Himalaya, mainly on the results of field research on two glaciers in Nepal Himalaya. *Low Temperature Science, Series A, 25*, 197–218.

Webster, P. J., Magana, V. O., Palmer, T. N., Shukla, J., Tomas, R. A., Yanai, M., & Yasunari, T. (1998). Monsoons: Processes, predictability, and prospects of prediction. *Journal of Geophysical Research, 103*, 14451–14510.

Webster, P. J., Andrew, W. M., Loschnigg, J. P., & Leben, R. R. (1999). Coupled ocean-temperature dynamics in the Indian Ocean during 1997–98. *Nature, 40*, 356–360.

Wild, M. (2009a). Global dimming and brightening: A review. *Journal of Geophysical Research, 114*, D00D16. doi:10.1029/2008JD011470.

Wild, M. (2009b). How well do IPCC-AR4/CMIP3 climate models simulate global dimming/brightening and twentieth-century daytime and night-time warming? *Journal of Geophysical Research Atmospheres, 114*, D00D11. doi:10.1029/2008JD011372.

Wild, M., Trussel, B., Ohmura, A., Long, C. N., Konig-Langlo, G., Dutton, E. G., & Tsvetkov, A. (2009). Global dimming and brightening: An update beyond 2000. *Journal of Geophysical Research, 114*, D00D13. doi:10.1029/2008JD011382.

Zhang, X., & Yang, F. (2004). *RClimDex (1.0) user manual*. Ontario: Environment Canada.

Zhang, Y., Wallace, J. M., & Battisti, D. S. (1997). ENSO-like variability: 1900–93. *Journal of Climate, 10*, 1004–1020.

http://www.springer.com/978-94-007-7338-7

Climate in Asia and the Pacific
Security, Society and Sustainability
Manton, M.; Stevenson, L.A. (Eds.)
2014, XVIII, 317 p. 45 illus., 41 illus. in color.,
ISBN: 978-94-007-7338-7